doi:10.1006/jmbi.2001.5062 available online at http://www.idealibrary.com on IDEAL® *J. Mol. Biol.* (2001) **313**, 593–614

JMB

Factorising Ligand Affinity: A Combined Thermodynamic and Crystallographic Study of Trypsin and Thrombin Inhibition†

Frank Dullweber[1], Milton T. Stubbs[1]*, Đorđe Musil[2], Jörg Stürzebecher[3] and Gerhard Klebe[1]*

[1]*Philipps-Universität Marburg Institut für Pharmazeutische Chemie, Marbacher Weg 6 D-35037 Marburg (Lahn) Germany*

[2]*Structural Chemistry Laboratory, AstraZeneca S-43183 Mölndal, Sweden*

[3]*Friedrich-Schiller-Universität Jena, Zentrum für Vaskuläre Biologie und Medizin Nordhäuser Straße 78 D-99089 Erfurt, Germany*

**Corresponding authors*

The binding of a series of low molecular weight ligands towards trypsin and thrombin has been studied by isothermal titration calorimetry and protein crystallography. In a series of congeneric ligands, surprising changes of protonation states occur and are overlaid on the binding process. They result from induced pK_a shifts depending on the local environment experienced by the ligand and protein functional groups in the complex (induced dielectric fit). They involve additional heat effects that must be corrected before any conclusion on the binding enthalpy (ΔH) and entropy (ΔS) can be drawn. After correction, trends in both contributions can be interpreted in structural terms with respect to the hydrogen bond inventory or residual ligand motions. For all inhibitors studied, a strong negative heat capacity change (ΔC_p) is detected, thus binding becomes more exothermic and entropically less favourable with increasing temperature. Due to a mutual compensation, Gibbs free energy remains virtually unchanged. The strong negative ΔC_p value cannot solely be explained by the removal of hydrophobic surface portions of the protein or ligand from water exposure. Additional contributions must be considered, presumably arising from modulations of the local water structure, changes in vibrational modes or other ordering parameters. For thrombin, smaller negative ΔC_p values are observed for ligand binding in the presence of sodium ions compared to the other alkali ions, probably due to stabilising effects on the protein or changes in the bound water structure.

Keywords: isothermal titration calorimetry; thermodynamics; X-ray crystallography; enthalpy-entropy compensation; drug design

Introduction

Binding affinity prediction is an essential element of structure-based drug design. While docking programs can now achieve a level of reliability that make them a viable tool for database screening of possible leads on the computer, the ranking of putative hits according to their expected affinity remains the most crucial step in this procedure. Despite an exponential increase in experimental structural data on protein-ligand complexes from X-ray crystallography and NMR, estimation of binding affinity from structural parameters is still not straightforward. Accordingly, there is an acute need for a better understanding of the thermodynamics determining affinity in the binding process.[1] For reasons of simplicity and tractability, conditions of equilibrium thermodynamics are generally assumed for complex formation. Binding affinity between a ligand and a protein is available from the association constant K_A. At equilibrium, this is related to the Gibbs free energy of binding ΔG, which is itself composed of an enthalpic (ΔH) and entropic ($-T\Delta S$) contribution.

In drug design, we are largely concerned with manifold non-covalent interactions between the

†We dedicate this paper to Professor Dr Hans-Beat Bürgi on the occasion of his 60th birthday.

Abbreviations used: ITC, isothermal calorimetry.

E-mail addresses of the corresponding authors: klebe@mailer.uni-marburg.de; stubbs@mailer.uni-marburg.de

0022-2836/01/030593–22 $35.00/0

ligand and the binding site residues of the protein. Of these, hydrogen bonding patterns are best characterised.[2] Such interactions will contribute to binding affinity provided stronger and more efficient hydrogen bonds are formed between functional groups of the ligand and the protein when compared to the isolated components in aqueous solution prior to complex formation. Efficient occupation of lipophilic regions of the binding pocket by shape-complementary ligand portions influences the affinity substantially, presumably as a result of the replacement or release of more or less ordered water molecules during ligand and protein desolvation. Loss or gain of degrees of molecular motion (as a consequence of complex formation, ligand immobilisation or solvent release and restructuring) modify the ordering parameters of the system.

Thermodynamically, these molecular parameters represent changes in enthalpy and entropy. As a consequence of enthalpy-entropy compensation,[3] an empirical linear relationship between the two thermodynamic entities, ΔG for a particular system remains rather constant at different temperatures, although there may be substantial individual changes in ΔH and $-T\Delta S$. Experimental approaches to determining the energetics of the binding process are based either on the temperature-dependent evaluation of binding affinity or on isothermal titration calorimetry (ITC).[4,5] Since the various entities to be measured are rarely independent of temperature, data collection performed by ITC at constant temperature is more appropriate and straight-forward.

Here, we report on a combined crystallographic and thermodynamic investigation of a series of ligands binding to thrombin and trypsin. We attempt to correlate structural features from the crystal data with thermodynamic data of the corresponding enzyme-inhibitor complexes examined by ITC. Trypsin-like serine proteinases are of interest as either potential targets in the blood coagulation system or as important model systems to study ligand-protein interactions and the structural and energetic features responsible for selectivity.

Despite the existence of numerous thrombin inhibitors with binding constants over the entire range from millimolar down to sub-nanomolar affinity,[6–8] a clear-cut correlation between structural or geometric features and increments in binding enthalpy or entropy remains to be established. We have investigated the thermodynamic properties of a series of closely related N^{α}-(2-naphthylsulphonyl)-L-3-amidino-phenylalanine derivatives 1a-1dAc (Figure 1). Furthermore, we have embarked upon a systematic study using several thrombin inhibitors (Figure 2), namely Napsagatran 2 (development abandoned; Roche), CRC220 3 (development abandoned; Chiron-Behring), inogatran 4 and melagatran 5 (preclinical/clinical trials; AstraZeneca).

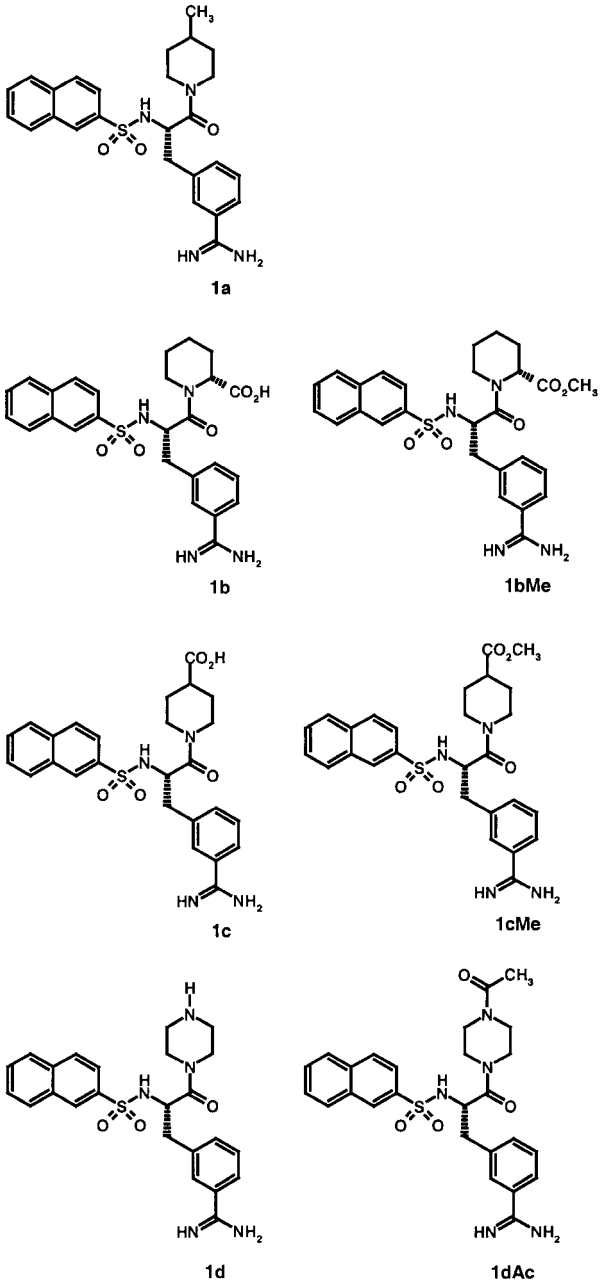

Figure 1. Chemical formulae of thrombin and trypsin inhibitors used in this study.

Thermodynamic background and calorimetric method

The simultaneous study of crystal and thermodynamic data allows the examination of molecular parameters responsible for binding. Gibbs free energy of binding is available from the equilibrium association constant K_A, which is the reciprocal of the dissociation constant K_D:

$$\Delta G = \Delta H - T\Delta S = -RT \ln K_A = RT \ln K_D \quad (1)$$

The inhibition constant K_i, related to the dis-

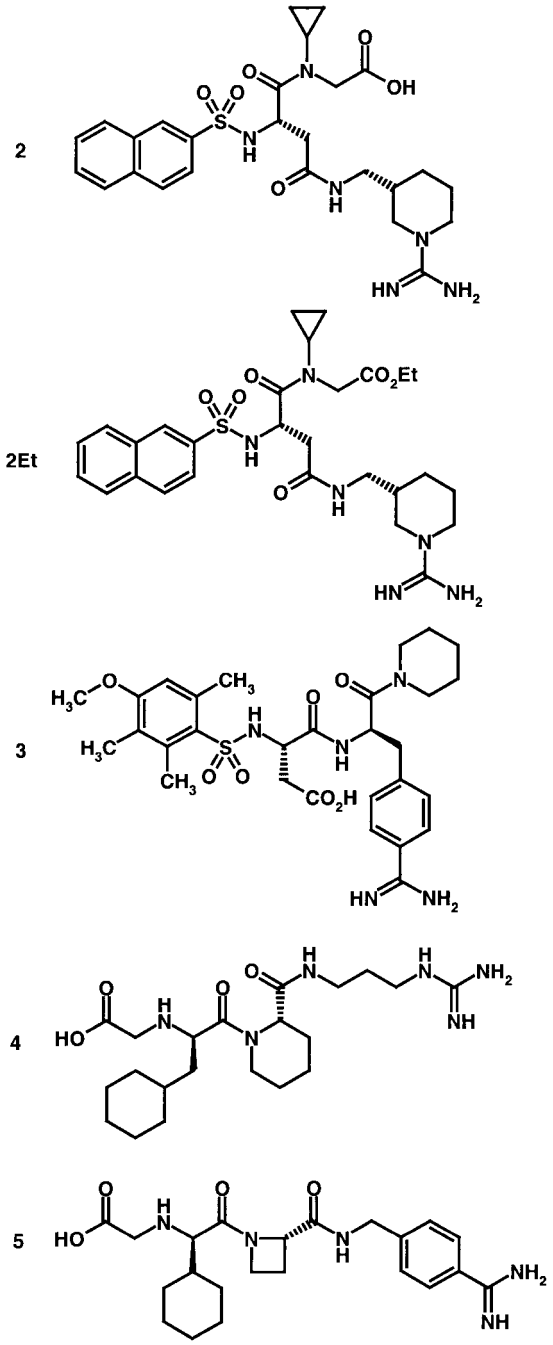

Figure 2. Chemical formulae of thrombin development compounds used in this study.

sociation constant K_D (Table 1), is derived from kinetic experiments that measure the competitive interference of an inhibitor with the cleavage rate of a chromogenic substrate. Collection of kinetic data at various temperatures allows the derivation of the enthalpy of binding from the plot of ln K_i *versus* $1/T$. Provided the enthalpy and the heat capacity ΔC_p are independent of temperature over the range studied, a linear correlation is found and ΔH is available from the slope $-\Delta H/R$ (van't Hoff plot). The entropic contribution to ΔG can then be calculated as $\Delta S = (\Delta H - \Delta G)/T$. However, ΔH tends to show a strong temperature dependence and non-linear van't Hoff plots are usually obtained.[9,10] For these reasons, methods measuring the generated or absorbed heat directly are more appropriate.

In isothermal titration calorimetry (ITC), a ligand is titrated step-wise into a sample solution of the macromolecule. The experiment is performed by keeping the temperature difference between the reaction and reference cell (usually filled with water) zero.[11] Figure 3 shows a typical result of an ITC measurement. Each peak in the upper part of the diagram corresponds to a single injection into the reaction cell, leading in this case to an exothermic reaction. The binding sites of the protein become saturated after several injections, so that the heat produced per injection gradually decreases. Plotting the heat produced for each injection step against the molar ratio between ligand and protein results in a sigmoidal dependence. The dissociation constant K_D can be computed from shape analysis of the titration curve.[12] Integrating over all heat pulses yields the total heat exchange of the binding reactions, after subtraction of the heat of dilution for all injection steps. In Figure 3, the heat changes observed after protein saturation originate from this heat of dilution.

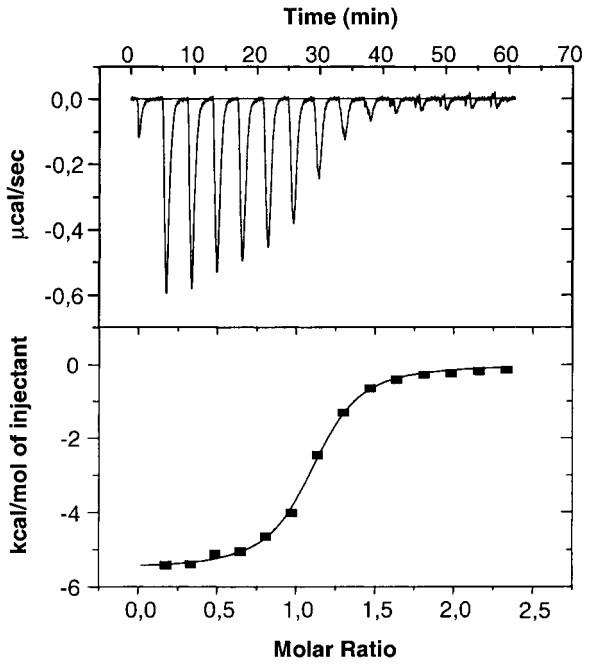

Figure 3. Typical result of an isothermal calorimetric titration of a low molecular weight inhibitor with trypsin. (a) The recorded change in heat is shown in units of µcal s^{-1} as a function of time for successive injections of the inhibitor. (b) Integrated heats (black squares) plotted against the molar ratio of the binding reaction. The continuous line represents the results of the non-linear least squares fitting of the data to a binding model.

Table 1. Dissociation constants towards trypsin measured either by binding kinetics or ITC

Substance	Kinetic K_i (nM)	Kinetic pK_i	Thermodynamic K_D (nM)	Thermodynamic pK_D
1a	42	7.3	39 ± 10	7.4
1b	660	6.2	264 ± 20	6.6
1bMe	1100	6.0	229 ± 80	6.6
1c	220	6.7	794 ± 137	6.1
1cMe	21	7.7	28 ± 5	7.6
1d	120	6.9	125 ± 15	6.9
1dAc	44	7.4	40 ± 7	7.4
2	11,600	4.9	2500 ± 438	5.6
2Et	30,000[a]	4.5	≈10,000	≈5
3	410	6.4	153 ± 21	6.8

[a] Hilpert *et al.*[18]

Comparing the binding constants obtained from curve fitting with those from reported kinetic data reveals an approximately 1:1 correlation (Table 1 and Figure 4).

If the titration experiment is performed at several temperatures, the change in heat capacity at constant pressure can be determined by plotting the observed heat against temperature. A linear relationship is usually observed within the temperature range 15 °C-35 °C, suggesting temperature independence of ΔC_p which can be calculated as:

$$\Delta C_p = (\Delta H_{T2} - \Delta H_{T1})/(T_2 - T_1) \qquad (2)$$

The ITC experiment records the total heat exchanged during the ligand-binding process. As a consequence, any additional reaction steps coupled with a transfer of heat will add to the intrinsic enthalpy of binding. Such supplementary effects must be characterised and corrected before a meaningful comparison of the enthalpic and entropic binding contributions within a series of ligands can be performed. Since proteins require particular buffer and salt conditions, both additives could influence the binding process. Accordingly, we performed our ITC experiments under several distinct buffer and salt conditions.

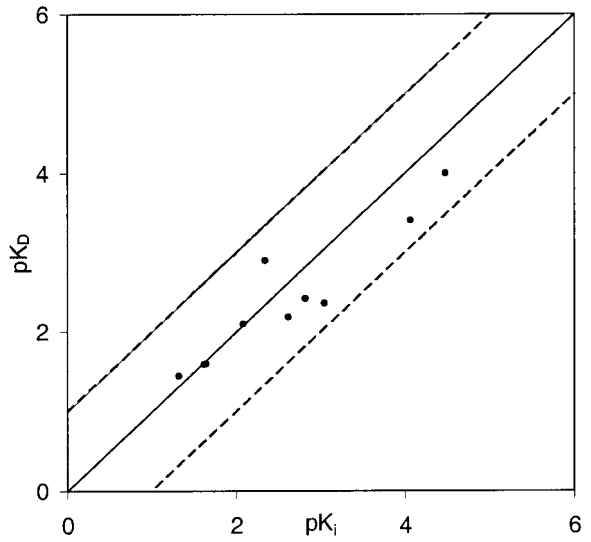

Figure 4. Correlation between kinetically measured inhibition constant pK_i and thermodynamically recorded dissociation constant pK_D (regression coefficient $r^2 = 0.88$) (Table 1).

Change of protonation upon complex formation

Proteins are usually studied under buffer conditions of constant pH. The observed enthalpy of binding ΔH_{obs}, measured for a single ITC experiment, is composed of all heat effects including those produced by protonation or deprotonation of the buffer during binding. This effect occurs if binding is coupled with a proton exchange between ligand L, protein P or complex PL and the buffer B:

$$P + L + nH^+ \rightarrow PL(nH^+) \quad \Delta H_{obs} \qquad (3)$$

The protons captured (or released) by the system during binding are released (or picked up) by the buffer substance BH^+, involving an ionisation enthalpy ΔH_{ion}:

$$BH^+ \rightarrow B + H^+ \quad \Delta H_{ion} \qquad (4)$$

Generally, the observed enthalpy of binding ΔH_{obs} is composed of the enthalpy ΔH_x (which is independent of the buffer system used) and a term which describes the deprotonation enthalpy ΔH_{ion} of the applied buffer:

$$\Delta H_{obs} = \Delta H_x + n\Delta H_{ion} \qquad (5)$$

where n is the number of protons released ($n > 0$) or captured ($n < 0$). If $n = 0$, binding shows no dependence on the buffer system and no protons are exchanged.

If the ionizable ligand functional group exhibits a non-zero deprotonation enthalpy and protons are exchanged with the ligand ($n \neq 0$), this deprotonation enthalpy ΔH_i must be corrected from the enthalpy ΔH_x to obtain the intrinsic binding enthalpy ΔH_{bind}:

$$\Delta H_{bind} = \Delta H_x + n\Delta H_i \qquad (6)$$

Although the binding affinity may well be inde-

pendent of the applied buffer conditions, the measured enthalpy might vary considerably.

Data set of ligands studied

We selected two series of inhibitors for detailed crystallographic and thermodynamic analysis. The first set comprises a congeneric series of seven *N*(2-naphthylsulphonyl)-L-3-amidino-phenylalanine derivatives 1a-1dAc substituted at the terminal peptide bond by different six-membered heterocycles, the second is composed of five development compounds 2-5 from different companies (Figures 1 and 2). Both sets of inhibitors were studied with respect to binding to bovine β-trypsin and α-thrombin; for the latter, crystallographic studies were performed on human α-thrombin, whilst thermodynamic measurements were made using bovine α-thrombin.

Results

Crystal structures with trypsin

Binding of compounds 1b, 1cMe, 1d, 1dAc

First, we will describe some basic features shared by the complexes of 1b, 1cMe, 1d and 1dAc with trypsin (Figures 5 and 6). All bind similarly to N^{α}-tosyl-3-amidino-phenylalanine-piperidide (3-TAPAP) (PDB code 1PPH)[13,14] with the basic benzamidino group buried deeply in the S1 specificity pocket. The amidino moiety (N1, N2; for nomenclature see Table 2) forms a nearly symmetric salt bridge with the carboxylate of Asp189. It is further stabilised by hydrogen bonds to the carbonyl group of Gly219 and the hydroxyl group of Ser190, which is itself stabilised by a hydrogen bond to a deeply buried water molecule (W407).

A short β-ladder is formed by hydrogen bonds between the amino (N3) and carbonyl (O3) groups of the central amidinophenylalanyl moiety and backbone oxygen and nitrogen of Gly216. One of the two sulphonyl oxygen atoms (OS1) is hydrogen bonded to Gly219N, forming together with the adjacent amidino nitrogen and Gly219O a second short β-ladder. The N-terminal naphthylsulphonyl group is buried in the S3/S4 pocket, with the ring system perpendicular to the indole moiety of Trp215; the C-terminal aliphatic ring occupies the S2 pocket almost parallel to the naphthyl moiety and the imidazole ring of His57.

Superposition of the complexes (Figure 6) based on a least squares fit of the catalytic amino acids His57, Asp102 and Ser195 and residue Asp189 of trypsin reveals negligible differences in the orientations of the benzamidine and C-terminal aliphatic ring of the four inhibitors. The orientation of the N-terminal naphthylsulphonyl group shows only a slightly altered binding mode for 1b, possibly as a result of the different crystal form adopted by this complex, leading to deviating packing patterns and steric crowding at the naphthyl ring. The hydrogen-bonding network and the buried surface area remain unchanged.

The electron density of the C-terminal ring of 1b (Figure 5(a)) is well defined and smaller *B* factors can be attributed to the ring atoms compared to the other complexes. One of the two oxygen atoms of the 2-carboxylate group of 1b forms hydrogen bonds to the hydroxyl group of Ser195 (2.9 Å) and to a sterically restricted water (W505; 2.7 Å) which is fixed by three further hydrogen bonds to Ser195OG, Gly193N and Gln192OE (or Gln192NE). The carbonyl group next to the C-terminal ring of 1cMe and 1dAc forms an additional hydrogen bond to Ser96O mediated by a water molecule. Compound 1d shows no additional hydrogen bond. The amino group of its piperazide moiety is 4.5 Å apart from the imidazole ring of His57.

The solvent structure is more or less conserved in all the structures described. Although the low resolution of 1dAc in complex with trypsin prevents location of the water molecule W407, residual electron density suggests that it is indeed present. The X-ray structures of 1cMe, 1d and 1dAc show a sulphate ion next to Ser195OG at the position occupied in 1b by the carboxylate group, but there is no direct interaction between sulphate ion and ligand. An overview of all hydrogen bonds for 1b, 1cMe, 1d, 1dAc and 3 is shown in Table 2.

Binding of compound 3

This compound[15] binds to trypsin (Figure 5(b) and Table 2) in a fashion similar to the archety-

Table 2. Selected hydrogen bond distances in complex with trypsin

	1b	1cMe	1d	1dAc	3
N1-Asp189 OD1	2.9	2.7	2.6	2.8	2.7
N2-Asp189 OD2	3.1	3.1	3.0	3.0	2.9
N1-Gly219 O	2.7	2.7	2.8	2.8	2.8
N2-Ser190 OG	3.0	2.8	2.6	2.7	2.9
N2-W407	2.9	2.9	3.1	-[a]	2.8
W407-Ser190 OG	2.9	3.0	3.3	-[a]	3.0
N3-Gly216 O	2.8	2.9	2.7	2.8	2.8
O3-Gly216 N	3.1	3.2	2.9	3.1	3.2
OS1-Gly219 N	2.8	2.9	2.9	2.9	-

[a] The water molecule W407 was not observed in this structure due to low resolution.

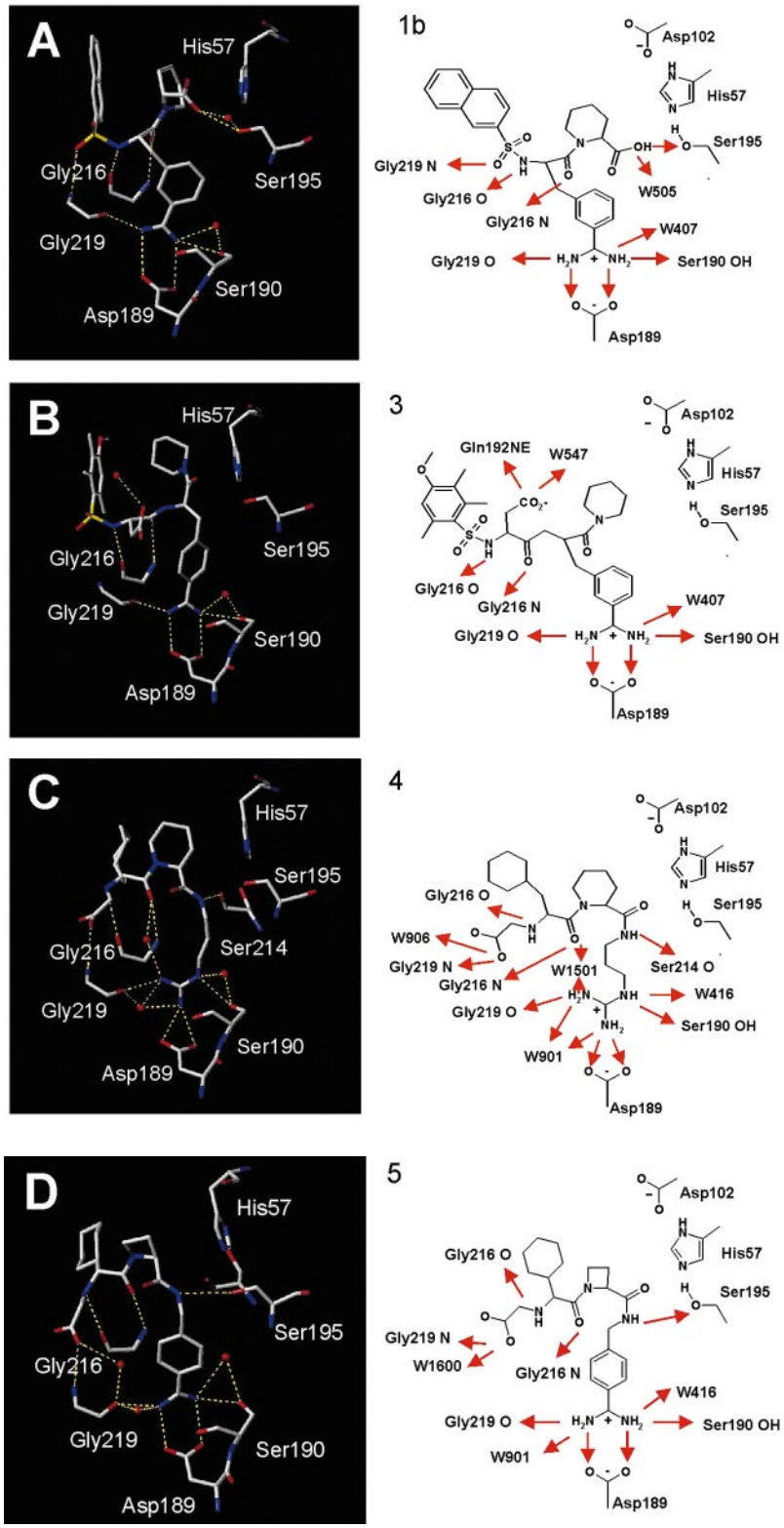

Figure 5. Observed binding modes and hydrogen bonding networks of compounds 1b (a), 3 (b) 4 (c) and 5 (d) for binding to bovine β-trypsin.

pal trypsin/thrombin inhibitor N^{α}-(2-naphthylsulphonylglycyl)-4-amidino-phenylalanine-piperidide (NAPAP) (PDB code 1PPC),[13,14] with the benzamidino moiety (N1, N2) binding similar to that of 1b, 1cMe, 1d and 1dAc in trypsin. All described interactions and the aforementioned conserved water W407 are also found in this complex. One favourable short β-ladder is formed by two hydrogen bonds between the amino (N3) and the carbonyl (O3) group of the central aspartyl residue of the inhibitor, and Gly216N and Gly216O of trypsin. One of the

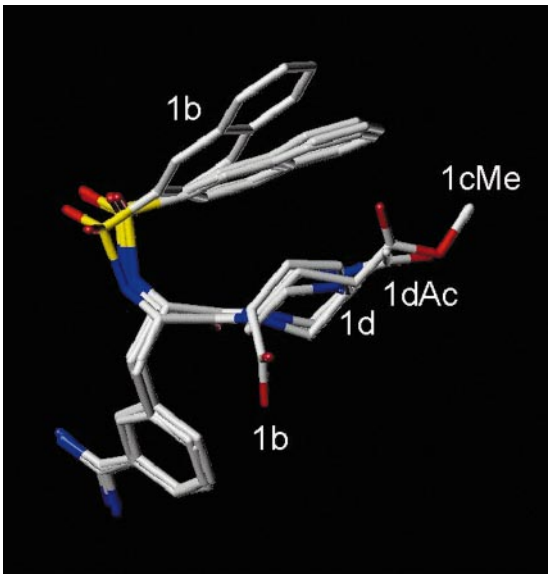

Figure 6. Mutual alignment of inhibitors 1b, 1cMe, 1d and 1dAc. The inhibitors were superimposed using the atoms of the amino acid residues His57, Asp102, Asp189 and Ser195 of trypsin. The position of the naphthyl group of 1b deviates from those of the remaining three inhibitors as a result of packing effects in this crystal form (co-crystal).

two carboxylate oxygen atoms of the ligand's central aspartate forms a weak hydrogen bond to Gln192NE (2.9 Å) and water W547. The oxygen atoms of the sulphonyl group are oriented away from the trypsin surface, exposed to bulk water as is the carboxylate group of the inhibitor. The C-terminal piperidine ring is neatly buried between the inhibitor's N-terminal phenyl and the imidazole ring of His57. The N-terminal phenyl ring occupies the hydrophobic aryl binding site (S3/S4 pocket). The electron density for all four substituents at the phenyl moiety is well defined, indicating a firm immobilisation of the N terminus near Trp215.

Binding of compound 4

Compound 4[17] shows a binding mode distinct to that of the benzamidino derivatives (Figure 5(c)). The guanidino group occupies the S1 specificity pocket in such a way that only one of its terminal nitrogen atoms (NH1) forms bifurcated hydrogen bonds to the two carboxylate oxygen atoms of Asp189 (single N-twin O contact). Furthermore, it is hydrogen bonded to a water molecule (W901; 3.0 Å) which itself forms a hydrogen bond to Asp189OD and a weak interaction to Gly219O (3.2 Å). The second terminal nitrogen (NH2) forms a contact *via* the same water molecule (2.9 Å) to Gly219O and a direct hydrogen bond to Gly219O (2.7 Å). This sophisticated hydrogen bond network of the two guanidino nitrogen atoms is completed by a further contact to a water molecule (W1501; 2.7 Å) which mediates an interaction to the carbonyl group (3.1 Å) of the ligand's cyclohexylalanyl residue. The third nitrogen of the guanidino group forms two hydrogen bonds, one directly to the hydroxyl group of Ser190 (2.8 Å) and a second *via* a water molecule (W407, 3.0 Å, stabilised by another contact to Val227O) to this hydroxyl group, similar to the binding described for the benzamidino residues of the other inhibitors. The fourth nitrogen stabilises the aliphatic carbon chain through a hydrogen bond to Ser214O (2.7 Å).

Whereas the electron density of the piperidine ring, buried in the S2 pocket (similarly to C-terminal ring described above), is well defined, the higher *B* factor attributed to the cyclohexyl ring suggests some residual motion of the moiety in the S3/S4 pocket.

A short β-ladder is formed *via* two weak hydrogen bonds between the amino and carbonyl group of the central cyclohexylalanyl moiety and trypsin atoms Gly216O and Gly216N. The electron density of the carboxylate of the terminal glycine is well-defined and orients away from the binding site toward the bulk solvent. One of its oxygen atoms forms hydrogen bonds to Gly219N and a water molecule W906.

Binding of compound 5

The benzamidino residue of 5[16,17] binds to Asp189 similar to the above-described benzamidino derivatives (Figure 5(d)). The electron density of the azetidine ring, buried in the S2 pocket, is well defined, similar to that of the piperidine ring of 4, whereas the cyclohexyl ring, lacking a firm anchoring group, appears to exhibit residual mobility in the S3/S4 pocket according to a less well defined electron density.

A short β-ladder is formed *via* two weak hydrogen bonds between the amino and carbonyl group of the central cyclohexylglycyl moiety and Gly216O and Gly216N (3.0 and 3.3 Å). One of the terminal carboxylate oxygen atoms is hydrogen bonded to Gly219N and *via* a conserved water molecule (W1600; 3.0 Å) to Gly219O (3.2 Å). The water molecule (W1501) which mediates intramolecular hydrogen bonds in the case of 4 is displaced by the sterically more demanding phenyl ring of the benzamidino group in 5 compared to the less restrictive aliphatic carbon chain in 4.

Crystal structures with thrombin

Binding of compound 2 to thrombin

Compound 2 is a highly selective thrombin inhibitor. The coordinates of the complex of 2[18] with human α-thrombin have been kindly provided by Hoffmann-La Roche (Basel, Switzerland); however, since the structure will be discussed with respect to its thermodynamic properties (*vide infra*) its binding mode will be described shortly (Figure 7(a)). The two terminal nitrogen atoms of

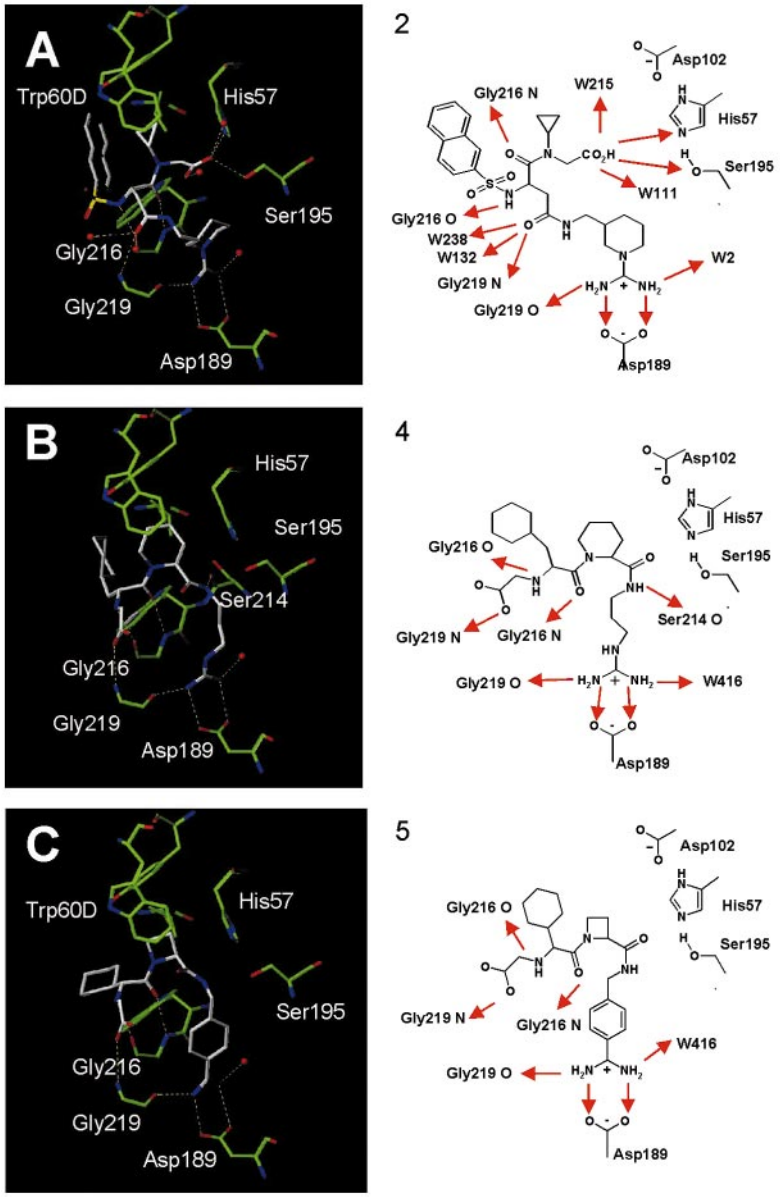

Figure 7. Observed binding modes and hydrogen bonding networks of compounds 2 (a), 4 (b) and 5 (c) to human α-thrombin.

the amidinopiperidyl group form a nearly symmetric salt bridge to the side-chain carboxylate of Asp189 (2.8 and 2.9 Å). They are further stabilised by contacts to the carbonyl oxygen of Gly219 (2.9 Å) and a conserved water molecule W2 (2.8 Å), which forms a further hydrogen bond to Phe227O. Ser190 in trypsin is replaced by Ala190 in thrombin, accordingly no additional hydrogen bond can be realised.

A short β-ladder is formed by the amino and carbonyl group of the central aspartyl residue with Gly216N and Gly216O (3.0 and 2.7 Å). The side-chain carboxylate of this aspartyl residue is further hydrogen bonded to Gly219N (3.2 Å). The two oxygen atoms of the sulphonyl group are oriented away from the binding site towards bulk water. The aromatic naphthyl system occupies the S3/S4 pocket whereas the *N*-cyclopropyl substituent is buried in the hydrophobic S2 pocket of thrombin.

The carboxyl group of the N-substituted glycine exhibits additional favourable contacts. One of its oxygen atoms forms two hydrogen bonds to the residues of the catalytic triad Ser195OG (2.7 Å), His57NE (2.7 Å) and a further one to a water molecule W111, whereas the second oxygen is hydrogen bonded to another water molecule W215.

The superposition (Figure 8) of this thrombin complex with the trypsin complex of 1b (superimposing the atoms of the catalytic triads His57, Asp102, Ser195 and Asp189) reveals that the carboxylate groups of both inhibitors occupy similar spatial regions adjacent to the hydroxyl group of the catalytic Ser195.

Binding of compound 4 to thrombin

The overall binding mode for this inhibitor in thrombin is similar to that described above in tryp-

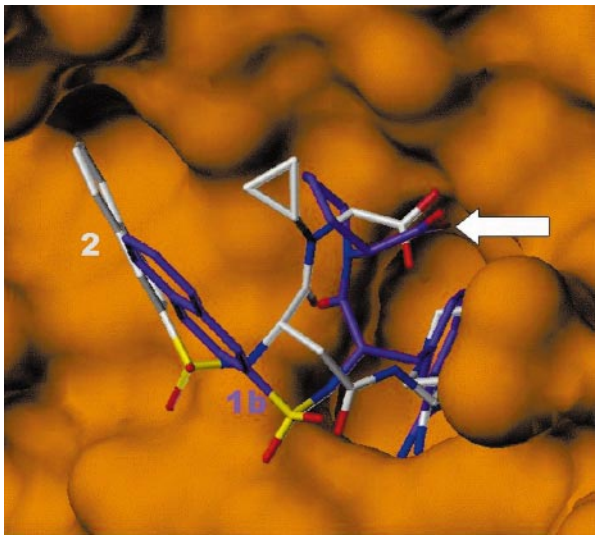

Figure 8. Alignment of inhibitors 1b (blue) and 2 (white). Trypsin shown by its solvent accessible surface. The inhibitors were superimposed using the atoms of amino acid residues His57, Asp102, Asp189 and Ser195 of trypsin or thrombin, respectively. Arrow indicates the location of the carboxylic groups.

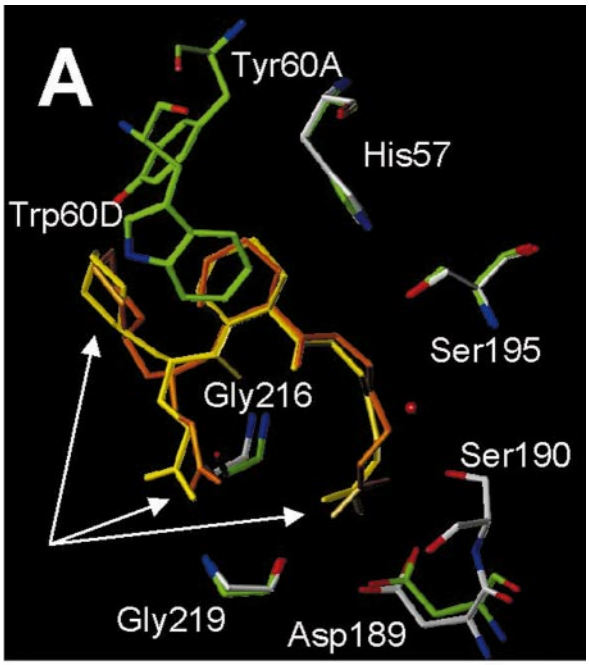

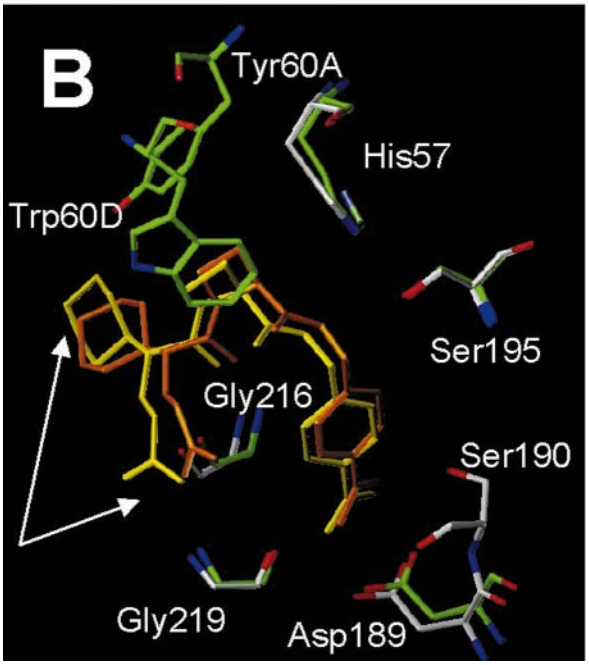

Figure 9. Overlays in trypsin (yellow/white) and thrombin (orange/green) of 4 (a) and 5 (b); white arrows highlight the differences in binding mode observed in trypsin and thrombin. In addition to the difference in binding of the guanidino group in trypsin and thrombin (4(a)), both 4 and 5 show similar changes in orientations of the cyclohexyl groups, presumably due to better packing within the aryl binding site of thrombin (Trp60D, Tyr60A and Leu99), and a concomitant rearrangement of the carboxylic acid groups.

sin; small yet significant differences are observed, however (Figures 7(b) and 9(a)). In contrast to the single N-twin O interaction between the guanidino function of 4 and the carboxylate side-chain of Asp189, the terminal nitrogen atoms NH1 and NH2 form a symmetric salt bridge with the carboxylate group, and NH1 makes hydrogen bonds with Gly219O and water molecule W524; thus the interactions of the terminal amidino function are identical to those observed for the benzamidine groups described above. As a consequence, no ''bridging'' water molecule is found equivalent to W1501 in trypsin. Outside the S1 pocket, the inhibitor is stabilised by similar hydrogen bonds to those observed in the trypsin structure; N^{α} of the arginine analogue makes an additional hydrogen bond (3.2 Å) to Ser195OG. The piperidine and cyclohexyl groups of the inhibitor occupy the aryl-binding site formed by the 60 loop and Ile99. The N-terminal carboxylate group has a slightly different orientation to that seen in the trypsin complex; in this case, O1 makes a hydrogen bond with Gly219O, while O2 contacts W501 (2.9 Å), which itself is located at the position of Gln192OE1 of the trypsin complex.

Binding of compound 5 to thrombin

Once again, the overall binding mode of 5 resembles closely that observed in the trypsin complex (Figures 7(c) and 9(b)). Slight rearrangements in the hydrogen bond pattern are seen: NH1 makes contacts to Asp189OD1 (2.7 Å), Gly219O (2.9 Å) and Ala190O (3.1 Å), while NH2 approaches Asp189OD2 (2.9 Å) and solvent molecule W413 (2.9 Å). As seen in 4-thrombin, the amide group of the benzamidine moiety approaches Ser195OG (3.1 Å), and the azetidine and cyclohexyl groups occupy the aryl binding

site. Furthermore, the carboxylate group occupies a similar location to that in 4-thrombin; O1 makes hydrogen bonds to Gly219O (2.8 Å) and Gly216N (3.1 Å), while O2 makes no contacts to either the enzyme or ordered solvent.

Change of protonation states upon binding

To determine the enthalpy ΔH_x, isothermal titration experiments were carried out at pH 7.8 in buffers of distinct deprotonation enthalpies:[19,20] pyrophosphate ($\Delta H_i = 5.12$ kJ/mol), Hepes ($\Delta H_i = 21.07$ kJ/mol), Tricine ($\Delta H_i = 31.97$ kJ/mol) and Tris ($\Delta H_i = 48.07$ kJ/mol). Figure 10 shows the dependency of ΔH_{obs} on deprotonation enthalpy ΔH_{ion}.

Binding enthalpies ΔH_{obs} of 1b, 1d and 2 to trypsin are dependent on the applied buffer (Table 3). Upon complex formation, one proton is transferred from the buffer to 1b and 2, whereas ''0.53 proton'' is released upon binding of 1d. Napsagatran 2 shows a similar behaviour upon complex formation with thrombin (Table 4). No dependency on the buffer conditions was recorded for the remaining inhibitors.

In order to obtain a reasonable estimate of the heats involved, we measured the heat of deprotonation of the reference compounds *N*-acetylglycine (mimicking the carboxylic group of 2), *N*-acetylpiperidine-2-carboxylic acid (*N*-acetylpipecolinic acid) (resembling the carboxylic group of 1b) and N-acetylpiperazine [imitating the amino group of 1dAc] (see Discussion). In agreement with the very small heat of ionisation found for acetate buffer of 0.4 kJ/mol,[19] the carboxylic groups of *N*-acetylglycine and *N*-acetylpiperidine-2-carboxylic acid also show a small deprotonation heat of approximately 0.84(±0.34) kJ/mol or 2.26(±0.56) kJ/mol, respectively. Thus, the contributions for 1b and 2 arising from the buffer and the ligand's carboxylic group must also be considered as superimposed on the total measured heat (Table 5). Similarly for 1d, the partial protonation of the piperazide moiety in water ($n = 0.53$) has been corrected in addition to the buffer correction (here the buffer reaction is exothermic) using the deprotonation enthalpy

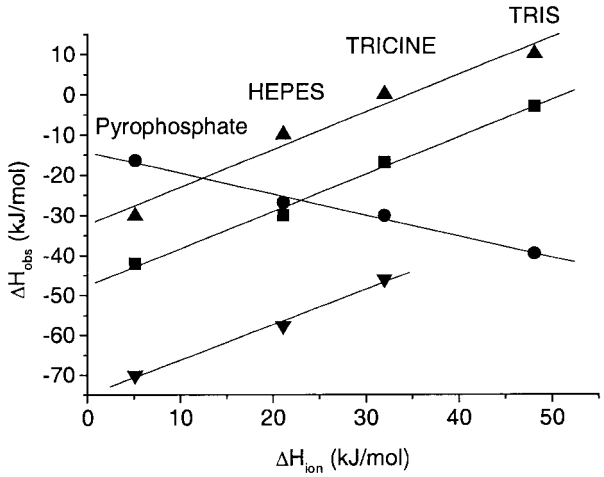

Figure 10. The observed enthalpy ΔH_{obs} for ligand binding as a function of the deprotonation enthalpy ΔH_i of the applied buffer for bovine β-trypsin and bovine α-thrombin. The slope of the linear regression yields the number of protons captured during the binding reaction and the intercept on the *y* axis shows the enthalpy of binding ΔH_x corrected for the deprotonation enthalpy of buffer. (■) 1b-trypsin; (●) 1d-trypsin; (▲) 2-trypsin, (▼) 2-thrombin. ΔH_{obs} of 2 for binding to thrombin in Tris buffer solution could not be determined.

measured for the amino group of the model compound *N*-acetylpiperazine of 35.16(±0.98) kJ/mol (Table 5). Assuming that no further heat-absorbing or generating steps are overlaid on the binding process, the values ΔH_{bind} (Table 5) correspond to the net binding reaction of the different ligands at 25 °C.

Decomposition of heat effects into enthalpic and entropic contributions

The values for ΔG were taken from the ITC experiment[12] except for thrombin inhibition of 2, 2Et, 3, 4 and 5. In these latter cases, the high affinities hamper a reliable shape analysis of the titration curve to determine ΔG. Thus, ΔG was calculated from the published kinetically determined

Table 3. Observed thermodynamic data for trypsin binding

Compound	ΔH_{obs} (kJ mol^{-1})	$-T\Delta S$ (kJ mol^{-1})	K (10^6 M^{-1})	ΔG (kJ mol^{-1})
1a	−27.1 ± 1.1	−15.4 ± 1.3	27.8 ± 7.0	−42.5
1b	*−42.0 ± 0.5*	*5.6 ± 0.5*	2.44 ± 0.19	−36.4
1bMe	−16.9 ± 0.8	−20.6 ± 1.2	3.11 ± 1.10	−37.0
1c	−26.8 ± 0.8	−8.7 ± 0.9	1.68 ± 0.29	−35.5
1cMe	−39.6 ± 1.0	−4.0 ± 1.1	44.0 ± 8.1	−43.6
1d	*−16.4 ± 1.0*	*−24.4 ± 1.3*	14.2 ± 5.0	−40.8
1dAc	−34.4 ± 0.8	−8.2 ± 0.9	30.3 ± 5.2	−42.7
2	*−10.0 ± 0.9*	*−1.9 ± 1.0*	0.40 ± 0.07	−32.0
3	−24.7 ± 1.2	−10.6 ± 1.2	5.22 ± 0.70	−38.3

Thermodynamic values were measured in pyrophosphate buffer (for details see Experimental Section and Methods).Values in italic for 1b, 1d and 2 are still affected by overlaid protonation steps and must be corrected for ionisation enthalpies. The corrected values of ΔH_{bind} are shown in Table 5.

Table 4. Observed thermodynamic data for thrombin binding

Compound	ΔH_{obs} (kJ mol^{-1})	$-T\Delta S$ (kJ mol^{-1})	K_i (nM)	ΔG (kJ mol^{-1})
2	*−70.0 ± 2.1*	*17.8*	0.7	−52.2
2Et	−24.4 ± 0.9	−15.9	86[a]	−40.3
3	−48.5 ± 1.0	−0.7	0.5	−49.2
4	−57.8 ± 2.0	10.0	4.2	−47.8
5	−37.0 ± 1.2	−10.9	4[b]	−47.9

Values are for bovine α-thrombin except [a18, b16] (both human α-thrombin). Thermodynamic values were measured in pyrophosphate buffer (for details see Experimental Section and Methods). Values in italic for 2 are still affected by overlaid protonation steps and have to be corrected for ionisation enthalpies. The corrected values of ΔH_{bind} are shown in Table 5.

binding constant. Entropic terms $-T\Delta S$ were computed using ΔG and the corrected ΔH_{bind} values (Tables 3-5) from the ITC experiment.

Within the congeneric series 1a-1dAc, ΔG covers a range from −43.6 up to −35.5 kJ/mol (Table 3). These ΔG values decomposed into varying ΔH and $-T\Delta S$ portions, mostly with a larger enthalpic contribution at 25 °C.

Heat capacity changes

Titration experiments performed at different temperatures reveal that the enthalpies of binding to thrombin and trypsin depend strongly on temperature, indicating large negative heat capacity changes upon binding (Tables 6 and 7). Since the relationship is linear, the assumption of a constant heat capacity change in the investigated temperature range is justified.

As the Gibbs free energy ΔG is temperature-independent (Table 8), the temperature dependency of ΔH must be compensated, so that the large negative heat capacity change also reveals a strong temperature dependence of ΔS.[3] As temperature increases, the binding process becomes increasingly exothermic (''enthalpy-driven'') and entropically less favourable.

Dependency on the applied salt conditions

We also investigated whether the concentration and the composition of the added salts have any influence on the observed thermodynamic parameters. For these studies we selected 2 and 3.

Variation of added polyethylene glycol 8000 concentration showed no alteration of the measured enthalpy values, whereas the variation of the sodium concentration resulted in different enthalpies ΔH for the same protein-ligand complex in the case of thrombin. We varied the sodium chloride concentration from 0 mM up to 900 mM in steps of 50 mM. Only measurements performed in the absence of sodium chloride showed deviating values; once sodium chloride was present above a concentration of 50 mM, no further concentration dependency on the added sodium chloride could be detected. In a further step, we exchanged sodium chloride by the chlorides of lithium, potassium, rubidium and caesium. Enthalpies measured in the presence of sodium chloride showed significant differences compared to all other measurements recorded in the absence of sodium chloride (Figure 11). Analogous studies with trypsin revealed no such effect.

Sodium dependence of thrombin resulting in distinct heat capacities

We found significant differences in the heat capacity changes upon binding of the low molecular weight inhibitors 2, 2Et, 3, 4 and 5 to thrombin depending on the presence of different monovalent cation in the buffer used. The ΔC_p values detected in the presence of rubidium chloride (as well as lithium, potassium and caesium) are about 1.2-1.4 times those observed in the presence of sodium chloride (Table 7). The absolute differences are in the range between 0.42 and 0.87 kJ mol^{-1} K^{-1}. Once again, trypsin showed no such sodium dependency in the measured ΔC_p values (ΔC_p (NaCl/RbCl): 2 (−0.91(±0.19)/ − 1.12(±0.11)

Table 5. Thermodynamic data corrected for overlaid protonation steps

Compound	Enzyme	n	ΔH_x (kJ mol^{-1})	ΔH_i (kJ mol^{-1})	ΔH_{bind} (kJ mol^{-1})	$-T\Delta S$ (kJ mol^{-1})
1b	Trypsin	0.90 ± 0.06	−47.6 ± 1.9	2.26	−45.6	9.2
1d	Trypsin	−0.53 ± 0.04	−14.3 ± 1.3	35.16	−32.9	−7.9
2	Trypsin	0.93 ± 0.12	−32.3 ± 3.6	0.84	−31.5	−0.5
2	Thrombin	0.88 ± 0.08	−75.1 ± 1.8	0.84	−74.4	22.2

Corrected intrinsic enthalpies ΔH_{bind} for binding of inhibitors to trypsin or thrombin. The constant n describes the number of protons captured from buffer and transferred to the complex (*vice versa* the protons released show a negative constant n). The enthalpy ΔH_x is the enthalpy corrected for this proton transfer from the buffer. The deprotonation enthalpy of the protonable group of the ligand is given by ΔH_i.[19] To determine the enthalpy of binding corrected for any overlaid effect from proton transfer this deprotonation enthalpy ΔH_i is subtracted from ΔH_x yielding ΔH_{bind}. ΔH_{bind} is identical to ΔH_{obs} reported in Table 3 for substances not involving any proton transfer(1a, 1bMe, 1c, 1cMe, 1dAc and 3 and in Table 4 for 2Et, 3, 4 and 5).

Table 6. Heat capacity changes and removed solvent accessible surfaces of inhibitors during binding reaction to trypsin

Compound	ΔC_p (kJ mol^{-1} K^{-1})	Removed SAS (Å^2)			ΔC_p (calc)	
		Total	Polar	Non-polar	$\Delta A_{np}^{(1)}$	$\Delta A_{np+p}^{(2)}$
1b	−2.59 ± 0.10	393	195	198	−0.33	−0.13
1bMe	−2.79 ± 0.11	436	220	216	−0.36	−0.14
1c	−2.26 ± 0.10	431	200	231	−0.39	−0.17
1cMe	−2.60 ± 0.12	448	200	248	−0.41	−0.19
1d	−2.20 ± 0.50	401	195	206	−0.34	−0.14
1dAc	−2.56 ± 0.09	430	198	232	−0.39	−0.17
2	−0.91 ± 0.19	497	217	280	−0.47	−0.22
3	−1.20 ± 0.15	477	204	273	−0.46	−0.22

The heat capacity changes ΔC_p (in kJ mol^{-1} K^{-1}) were measured in pyrophosphate buffer (for details see Experimental Section and Methods). The calculated surfaces are the solvent accessible surfaces (SAS) (Connolly surface with probe radius of 1.5 Å) removed during inhibitor binding to trypsin. The calculated polar surface includes the nitrogen and oxygen atoms with their hydrogen atoms. The calculated non-polar surface is the difference between the total surface and polar surface. ΔC_p(calc) (kJ mol^{-1} K^{-1}) was also calculated according to the change in non-polar surface area ($\Delta A_{np}^{(1)}$) according to Connelly & Thompson,[34] as well as the combined change in non-polar and polar surface ($\Delta A_{np+p}^{(2)}$) according to Spolar & Record.[37]

kJmol^{-1}K^{-1}); 3: (−1.20(±0.15)/ − 1.31(±0.22) kJmol^{-1}K^{-1})).

Discussion

Comparison of trypsin and thrombin complexes

We have noted previously that structural studies of benzamidine-based inhibitors in trypsin provide a reliable indication of binding modes for related serine proteinases.[21] This would also appear to be the case for 1a-1dAc; the crystal structure of 1a in complex with bovine ε-thrombin[22] reveals this inhibitor to bind almost identically to the related N^{α}-tosyl-3-amidino-phenylalanine-piperidide (3-TAPAP) (PDB code 1PPH). Furthermore, structural studies on inhibitor binding to human α-thrombin[23] and bovine ε-thrombin[24] reveal negligible differences in binding mode between the two species. Similarly, inhibition data show that the two thrombins display equivalent kinetic activities.[25] Accordingly, we assume identical binding to human/bovine thrombin for the other inhibitors described in this congeneric series.

Comparison of the binding of inhibitors 4 and 5 to trypsin and thrombin reveal equivalent locations of the ligands in both enzymes, although the solvent environment of the inhibitors is not conserved. Subtle differences are seen in the utilisation of interaction repertoires (Figure 9). Visual inspection of the structures shows that the most obvious differences are to be seen for the N-terminal cyclohexyl and carboxylate groups. The former is presumably influenced strongly through optimal burial within the aryl binding site of thrombin, which is open to bulk solvent in trypsin. We assume that optimisation of these interactions results in a slightly different organisation of the inhibitor backbone, causing the carboxylate group to adopt different hydrogen bonding partners. Further differences are noted within the primary specificity pocket, reflecting the presence of an additional hydrogen bonding partner in trypsin in the form of Ser190OG; this is particularly noticeable for the guanidino function of 4. What we appear to witness in these structures is the optimisation of a multitude of competing and complementary interactions, resulting in subtly different

Table 7. Heat capacity changes and removed solvent accessible surfaces of inhibitors during binding reaction to thrombin

Compound	ΔC_p (kJ mol^{-1} K^{-1})		Removed SAS (Å^2)			ΔC_p (calc)	
	With NaCl	With RbCl	Total	Polar	Non-polar	$\Delta A_{np}^{(1)}$	$\Delta A_{np+p}^{(2)}$
2	−2.31 ± 0.37	−3.14 ± 0.20	608	237	371	−0.62	−0.32
2Et	−2.07 ± 0.16	−2.51 ± 0.21	579	195	384	−0.64	−0.36
3	−2.77 ± 0.40	−3.64 ± 0.10	719	207	512	−0.86	−0.51
4	−2.22 ± 0.10	−2.64 ± 0.34	509	163	346	−0.58	−0.33
5	−2.28 ± 0.20	−2.84 ± 0.31	515	184	331	−0.55	−0.30

The heat capacity change ΔC_p (in kJ mol^{-1} K^{-1}) were measured for bovine α-thrombin in pyrophosphate buffer with 100 mM NaCl or 100 mM RbCl, respectively (for details see Experimental Section and Methods). The calculated surfaces are the solvent accessible surfaces (SAS) (Connolly surface with probe radius of 1.5 Å) removed during inhibitor binding to human α-thrombin. The calculated polar surface includes the nitrogen and oxygen atoms with their hydrogen atoms. The calculated non-polar surface is the difference between the total surface and polar surface. ΔC_p(calc) (kJ mol^{-1} K^{-1}) was also calculated according to the change in non-polar surface area ($\Delta A_{np}^{(1)}$) according to Connelly & Thompson,[34] as well as the combined change in non-polar and polar surface ($\Delta A_{np+p}^{(2)}$) according to Spolar & Record.[37]

Table 8. Inhibition constants determined in dependence of temperature and added salt

Salt			Temperature (°C)			
			26	30	35	40
2-trypsin	NaCl	K_i	11,600	16,900	18,500	29,200
		ΔG	−28.3	−27.7	−27.9	−27.2
2-trypsin	KCl	K_i	15,000	18,100	17,200	18,900
		ΔG	−27.6	−27.5	−28.1	−28.3
3-trypsin	NaCl	K_i	410	550	570	740
		ΔG	−36.6	−36.3	−36.8	−36.7
3-trypsin	KCl	K_i	560	790	790	650
		ΔG	−35.8	−35.4	−36.0	−37.0
2-thrombin	NaCl	K_i	0.71	0.78	1.21	1.29
		ΔG	−52.4	−52.8	−52.6	−53.3
2-thrombin	KCl	K_i	0.77	0.80	0.98	0.98
		ΔG	−52.2	−52.8	−53.1	−53.5
3-thrombin	NaCl	K_i	2.27	1.72	1.87	2.26
		ΔG	−49.5	−50.8	−51.5	−51.8
3-thrombin	KCl	K_i	1.97	2.47	2.23	2.00
		ΔG	−49.8	−49.9	−51.0	−52.1

Inhibition constants K_i ((M) with their corresponding Gibbs free energy ΔG (kJ/mol) of 2 and 3 at four different temperatures and applying two different cations.

binding modes which drive the selectivity of these ligands for their target proteins.

Changes in protonation

Increasing attention has been focussed on protonation and deprotonation steps during ligand binding.[26–31] We measured the pK_a values for all inhibitors 1a-5 (Table 9) by potentiometric titration. Napsagatran 2 exhibits three protonatable groups: a basic guanidino (pK_a = 12.25), a sulphonamide (pK_a = 10.12) and a carboxylate (pK_a = 3.40) group. One proton is captured upon binding to either trypsin or thrombin (Table 5); we assign this to the carboxylate group. In aqueous solution, the carboxylate is deprotonated at pH 7.8 (where the measurements were carried out) while the other groups are protonated. This is confirmed by the fact that ΔH_{obs} of the ethylester 2Et shows no dependency on the applied buffer upon complex formation. We assume a significant pK_a shift in 2 for the carboxylate from 3.4 to a value beyond 7.8 upon binding. In the crystal structure of 2, the carboxylate forms hydrogen bonds to the hydroxyl group of Ser195 (2.7 Å) and the imidazole nitrogen $N^{\varepsilon 2}$ of His57 (2.7 Å), and is deeply buried in the hydrophobic S2 pocket of thrombin.

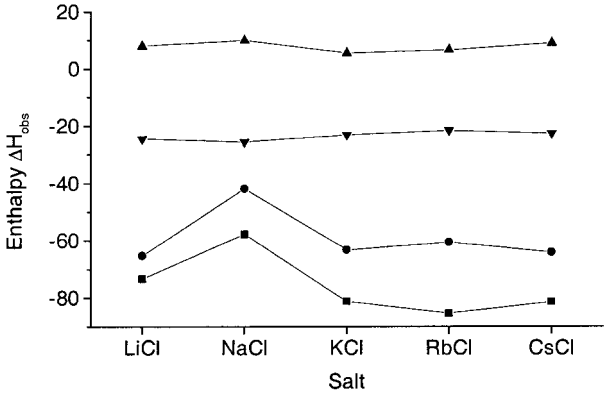

Figure 11. The observed enthalpy ΔH_{obs} as a function of the type of salt used for thermodynamic measurements for bovine β-trypsin and bovine α-thrombin. The composition of the buffer system was 50 mM Tris, 100 mM chloride salt, 0.1% polyethylene glycol 8000 (pH 7.8). (●) 2-thrombin; (■) 3-thrombin; (▲) 2-trypsin; (▼) 3-trypsin, values for 2 are not corrected for the overlaid protonation reaction; however, this is not important for a relative comparison of the salt effects.

Similarly 1b, with a free carboxylate group at the 2 position of the C-terminal piperidine ring, captures a proton upon binding (Table 5) whilst the methylester 1bMe maintains its protonation state. Not only do 1b and 2 possess similar protonatable groups, they position their carboxylates in very similar regions of the binding pocket (Figure 8). Due to a different orientation of the carboxylate group, however, no hydrogen bond is made with His57. The isomeric inhibitor 1c, with a 4-carboxylic group at the piperidine ring, adopts a very similar overall binding mode with respect to 1b, yet shows no buffer effect. In contrast to 1b, the carboxylate of 1c and the ester group of 1cMe make only van der Waals contacts to trypsin. No hydrogen bonds are formed for this group, and it is rather exposed to solvent.

This finding is mirrored by the compounds 3, 4 and 5, each with similar functional groups and a carboxylate group of comparable acidity. In each of these inhibitors, which show no buffer dependency, the discussed carboxylate groups are oriented away from the protein toward the bulk water. This completely different spatial location of the acidic group in 2 and 3 is shown in Figure 12.

Finally, inhibitor 1d releases a proton upon binding. The C-terminal piperazide amino group approaches His57 of trypsin. The protein environment has a clear impact on this functional group,

Table 9. Ionization constants (pK_a) of different ligand functional groups

Compound	Ionization constants (pK_a)		
1a	11.38	10.02	
1b	11.99	10.33	3.21
1bMe	11.71	10.26	
1c	11.78	10.20	4.17
1cMe	11.79	10.11	
1d	11.43	9.90	7.49
1dAc	11.54	9.91	
2	12.25	10.12	3.40
2Et	12.12	9.83	
3	11.57	10.67	3.84
4	≈12[a]	7.48	2.65
5	≈11.5[a]	7.95	2.51

[a] These values could not be determined with sufficient accuracy due to small amounts of substance.

whose pK_a value (7.49) is close to the pH of the applied buffer conditions. Upon binding, the amino group's pK_a value is shifted toward lower pH; inhibitor 1dAc does not alter its protonation state as the piperazine nitrogen is protected by an acetyl group. For 1d 0.53 mol protons per 1 mol substance were released upon binding (Table 5). This is in agreement with the results obtained from the Henderson-Hasselbalch-equation for a buffer of pH 7.8.

The most likely explanation for the observed change in protonation for certain compounds is the close approach of titratable groups of the inhibitor to the active site residues Ser195 and His57. Simple hydrogen bonding is neither necessary nor sufficient, as 1d (protonation change) makes no hydrogen bond, whilst 5 (no protonation change) does. Presumably for the latter compound, the pK_a value of the amide N^{α} group is too high to allow deprotonation. The exact source/destination for the transferred protons is not possible to ascertain; however, it is perhaps of significance that serine proteinases have evolved to shuttle protons between Asp102, His57, Ser195 and the substrate (the charge relay system).

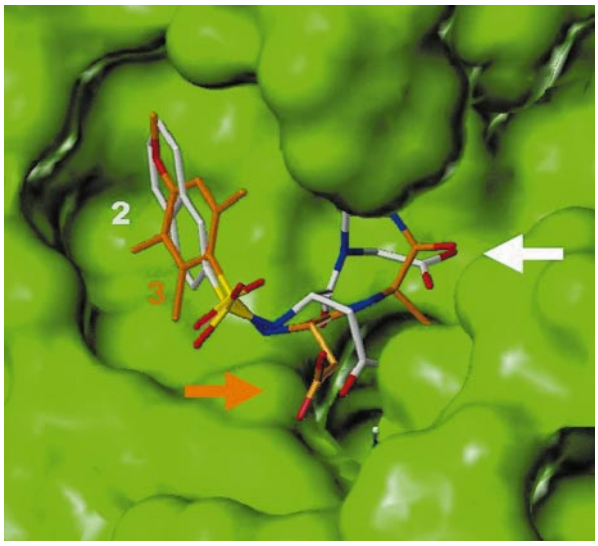

Figure 12. Alignment of inhibitors 2 (white) and 3 (orange). Human α-thrombin is shown by its solvent accessible surface. The inhibitors were superimposed using the atoms of amino acid residues His57, Asp102, Asp189 and Ser195 of trypsin or thrombin, respectively. Arrows indicate the location of the carboxylic groups.

Decomposition of heat effects into enthalpic and entropic contributions

The inhibitors studied here show wide variations in their enthalpic and entropic components on binding against trypsin (Table 3 and 5). Of particular interest are the congeneric pairs 1b/1bMe, 1c/1cMe, 1d/1dAc and 2/2Et, as they show quite different partitioning of ΔG into ΔH and $-T\Delta S$.

The reduced negative ΔH value of the acid 1c compared to the ester 1cMe presumably arises as a result of differences in solvation properties. In general, desolvation of an acid should be less favourable compared to an ester, in particular if there are no corresponding polar counter groups in the protein to compensate for lost interactions with the solvent. As a trade-off for this unfavourable inventory, we suggest that the exothermic binding enthalpy of 1c is more strongly reduced (losing solvent contacts to two polar carboxylate oxygens) compared to that of the ester 1cMe (possessing only the carbonyl oxygen as potential H-bonding partner).[32] As the small favourable entropic contributions are similar for both inhibitors, the differences in enthalpy result in different binding affinities.

In contrast, the acid 1b shows a stronger negative ΔH value compared to the ester 1bMe. In this case, the carboxylate of 1b gains a proton, so that the generated free acid forms a new hydrogen bond to Ser195. The ester cannot form an equivalent hydrogen bond. The similar ΔG values of the two inhibitors point to a compensation of the enthalpic and entropic contributions arising from the difference in H bond inventory.

We observe the same situation for the pair 2/2Et for binding to thrombin (Table 4 and 5). Once again, 2 gains a proton on binding, allowing the formation of a new hydrogen bond to the protein.

Thermodynamically, this is reflected in a stronger exothermic reaction compared to the ester 2Et. For both 1b/1bMe and 2/2Et, the entropic contributions differ significantly between acid and ester. At 25 °C, binding of the acids appears entropically disfavoured, whereas the ester binding is favourable. The formation of the hydrogen bond (leading to a higher enthalpic contribution) leads to a better immobilisation of the acids in 1b and 2, resulting in a decrease of the entropic component.

For the pair 1d/1dAc, not only do we observe similar values for ΔG, but also (after correction for protonation effects, cf. Tables 3 and 5) almost identical partitioning into ΔH and $-T\Delta S$. In each inhibitor (the unsubstituted piperazine 1d and the protected acetyl derivative 1dAc), only one polar atom is present in the C-terminal portion capable of forming hydrogen bonds. In the protein bound state, neither group possesses a suitable counter group from the protein; this uncompensated inventory must be reflected in an (in each case similar) unfavourable desolvation contribution.

Finally, the chemically related thrombin inhibitors 4 and 5, with similar K_i (and hence ΔG, Table 1) values, behave quite differently thermodynamically. Compared to 5, binding of 4 is entropically less favourable (Table 4). One contribution will be from the steric restriction incurred on binding of the flexible aliphatic arginine-like side-chain of 4, which is entropically less favourable than that for the conformationally restricted benzamidine moiety of 5. Furthermore, the local 2-fold symmetry axis of the *para*-substituted benzamidine moiety allows a residual jump-rotational ''disorder'' over two states in the complex that might also be entropically favoured.

Changes in heat capacity

In recent years, direct calorimetric measurements have shown that many processes involving proteins are accompanied by significant changes in heat capacity. Taking the complex as reference state, negative values for ΔC_p are usually obtained for protein-ligand complexes, i.e. the complex exhibits a smaller heat capacity than the sum of the separated components.[31] The heat capacity provides information on the dehydration of molecular portions at the interface to water. Heat capacity changes of protein unfolding are mainly governed by the hydrophobic effect and internal vibrational modes.[33–36]

Upon ligand binding, polar and non-polar functional groups are removed from bulk solvent conditions, leading to the release and restructuring of bound water molecules. At the interface of lipophilic molecular portions, the solvent water molecules must arrange in a more ordered fashion, so that release of the solute from water implies a transfer from a more to a less ordered state. The heat capacity change associated with complex formation has been interpreted previously as an indicator of change in water accessible surface area, and several empirical relationships have been derived.[34,37] Further evidence for the impact of the hydrophobic surface portions with respect to heat capacity changes has been reported by several authors.[35,38–45]

We calculated the buried surface area by removing the ligands from the determined crystal structures with the enzyme. Although this is not strictly the apo-form of the enzyme, we can justify the approximation as trypsin shows limited conformation variability in this region. Applying the above-mentioned empirical relationships to our trypsin inhibitors would give ΔC_p values between -0.33 and -0.47 kJ mol^{-1} K^{-1} (for removal of a non-polar surface[34] between 198 Å^2 and 280 Å^2; Table 6). Thus, only a fraction of the measured values (from -2.20 to -2.79 kJ mol^{-1} K^{-1}) can be explained. Inclusion of the contribution of the buried polar surface[37] results in an even larger discrepancy (Table 6). Moreover, the inhibitors exhibiting the largest surface buried upon binding (2 and 3) display less negative ΔC_p values.

What might be the reasons for the observed discrepancy? One problem may be the scaling of molecular surface contributions to ΔC_p derived for one class of molecules (protein-protein interactions) and transferred to another class (protein-ligand interactions). If this were the case, however, one would at least expect to see a correlation within the congeneric series 1a-1dAc (Table 6). As this is not really evident, we must seek alternative explanations. Similar discrepancies between calculated ΔC_p and experimentally observed values have been reported recently.[30,46] The changes in ΔC_p may arise from ordering phenomena related to the release or fixation of water molecules, the absorption or excitation of low frequency translational and vibrational modes or the immobilisation of conformational degrees of freedom. This concept is supported by the fact that 2 and 3, possessing the largest surface portions, show significantly smaller negative ΔC_p values compared to the congeneric series 1a-1dAc. The larger number of rotatable bonds in 2 and 3 may lead to increased flexibility of the ligands in solution and perhaps also in the binding site. Whether residual rigid body motions of the ligands in the complexes formed by trypsin with 1a-1dAc or those with 2 and 3 are better able to absorb low frequency vibrational modes is difficult to estimate; however, this aspect might be of significance for the absolute magnitude of ΔC_p.

A further point to bear in mind is that binding takes place in aqueous solution. An increase in temperature produces changes in both the ordering parameters of the surrounding solvent and in the conformational states of the molecules involved. These properties may result in a gain or loss of entropy. With increasing temperature, binding of 1a-5 becomes entropically less favourable. The release of water molecules from the binding site is entropically favoured; Dunitz[47] postulated an upper limit of about 40 J K^{-1} (mol water)$^{-1}$ as entropic gain for the release of a firmly fixed water

molecule. On the other hand, involvement of a water molecule in a contact mediating a hydrogen bond between protein and ligand will be penalised by a loss in entropy. Complex formation corresponds to a loss of translational, rotational and conformational entropy due to the loss of independent motion and ligand immobilisation. Depending on the strength of protein-ligand binding, this loss will be partially compensated by contributions arising from newly activated, heat absorbing vibrational modes of the formed complex. The various contributions are, depending on temperature, of different sign and size. They will compensate to some extent, as in the present examples and, to the best of our knowledge, for most protein-ligand binding processes in a way that for the total process a negative ΔC_p and thus a loss of entropy results with increasing temperature. If this holds true generally for a broad range of complex formations involving structurally quite distinct reaction partners, the role of the ubiquitously present and involved water may predominate.

Similar effects are reported by Liggins & Privalov,[46] who discuss the enthalpy and large negative heat capacity changes found for protein association with DNA in terms of dehydration of molecular groups that are removed from contact with water. As with our results, their ΔC_p values estimated from the surface portions buried upon binding cover only about half of the experimentally observed negative values. They propose that polar groups not completely dehydrated at the interface can still influence the state of water that has been removed in their vicinity, suggesting that polar interaction pairs created upon complex formation are not fully isolated from water and still affect the thermodynamic parameters of the system. Since these considerations would be valid for a large variety of molecules, they could explain the general underestimation of ΔC_p estimated solely from buried surface portions.

Heat capacity changes dependent of sodium ions

Thrombin specificity can be switched from procoagulant (i.e. fibrinogen as preferred substrate) to anti-coagulant (activation of Protein C) through the presence or absence of sodium.[48,49] Two sodium binding sites of thrombin have been determined in the presence of sodium and rubidium.[50,51] Although the kinetic parameters differ in the presence of Na^+ and Rb^+, no difference could be seen in the structures. In fact, thrombin appears to be a rather rigid enzyme, with minor variations in the 60 loop bordering the S2-pocket and aryl binding site[52] and the 148 loop. The one exception is in the thrombin(E192Q)-basic pancreatic trypsin inhibitor (BPTI) complex, in which an energetically unfavourable major rearrangement of the 60 loop is observed.[53] On the basis of thermodynamic data,[54] a large structural rearrangement has been proposed upon the binding of hirudin to thrombin, although structural data do not bear this out.[55,56]

Strongly altered heat capacity changes result for the binding to thrombin depending on the presence of sodium ions. This leads to an even larger discrepancy between measured ΔCp values and those calculated from the changed surface area (Table 7). In particular, it is difficult to explain the large difference between Na^+ and Rb^+, as there is no structural evidence for changes in surface area. As described above, the heat capacity changes are seriously underestimated from such an approach; clearly, a new theoretical framework is required to explain these results. Direct influence of the alkali ions on the inhibitor binding is unlikely, as the two sites are some 15 Å and 20 Å away from the thrombin active site. One possible explanation for the difference in ΔC_p on the binding of Na^+ *versus* Rb^+ may be a differential intrinsic stability of the cation bound enzymes, not detectable *via* crystallographic methods. Once again, rearrangements in the peripheral solvent structure may play a significant role in the magnitude of ΔC_p.

For the binding of a monovalent cation, electrostatic (i.e. enthalpic) effects are presumed to contribute a major part of the interaction. It would be interesting to see whether this binding also results in different ΔC_p values. However, since the binding constant of the ions is only in the millimolar range, a calorimetric quantification is beyond the experimental detection level of the ITC method.

Binding of hirudin and other large peptide-type ligands have been studied by means of van't Hoff analysis of kinetic data. Interestingly enough, no ΔC_p dependency on the presence of sodium *versus* rubidium ions could be detected.[54,57] Clearly, these larger systems also contain greater degrees of freedom, greatly reducing the significance of the ion effect. Our results on the binding of small molecule ligands do show, however, that sole consideration of the buried surface area leads to a serious underestimation of the ΔC_p value. On the basis of these findings, we suggest that large changes in ΔC_p do not necessarily equate to changes in surface area (and by implication conformational rearrangements), and that other factors such as solvent structure rearrangement and changes in degrees of freedom on ligand binding may be of considerable significance.

Conclusions

We selected isothermal titration calorimetry to measure directly a complete set of thermodynamic parameters for the binding of several low molecular weight inhibitors to trypsin and thrombin. In parallel, we determined the crystal structures of the complexes under consideration up to a resolution of 1.9 Å. Trypsin and thrombin are stable in the desired temperature range, well accessible and easy to purify in the required quantities. For both enzymes, a plethora of different inhibitors has been

collected due to intensive drug research programmes over the last years. Both enzymes have frequently been used for case studies in rational drug design.

Our experiments indicate that even in a series of congeneric ligands, significant changes of protonation states can occur. In retrospect, locally induced pK_a shifts should not be surprising, considering the well-established principles of nature to tailor the physicochemical properties of the 20 natural amino acids to meet the conditions required during enzyme catalysis. Likewise, ligand and protein functional groups can experience changes in protonation state upon complex formation. These steps are superimposed on the binding process and they involve additional heat effects due to protonation or deprotonation of functional groups either of the ligand, the protein or the buffer compounds. They must be determined and considered in the total heat measured in an ITC experiment before any conclusion can be drawn on the binding enthalpy ΔH and accordingly on the binding entropy ΔS. Similarly, the presence or absence of alternative ions can influence the decomposition of the interaction.

Once the different effects have been corrected for, trends in ΔH and $-T\Delta S$ can be interpreted in structural terms. An unbalanced hydrogen bond inventory between solvated and bound state is enthalpically unfavourable. A more restricted accommodation of the ligand in the binding site parallels a loss in entropy. For all ligands investigated, a strong negative heat capacity change is detected. Thus, binding becomes more exothermic and entropically less favourable with increasing temperature. Due to a mutual compensation of enthalpic and entropic effects, which leaves ΔG of the system virtually unchanged, the relative ratio of a $\Delta H/T\Delta S$ decomposition will depend on the temperature selected for the experiment. This must be considered in the discussion of a particular binding process as being enthalpy or entropy-driven, in particular if the data have been collected at room temperature but the results are applied to physiological conditions.

Until now, negative heat capacity changes have been interpreted only on the basis of removal of hydrophobic surface portions of the protein or ligand from water exposure. A larger than expected change in ΔC_p value has thereby been associated with increased hydrophobic surface area exposure and thus with structural rearrangements on binding. However, applying established correlations to our test examples explain only part of the observed ΔC_p. We suggest that a pure correlation between buried surface area and ΔC_p may be an oversimplification, and that further contributions arising from modulations in the local water structure, dehydration of functional groups, changes of vibrational modes or other ordering parameters of the system are responsible for the observed strong negative heat capacity changes.

Finally, the obtained dependencies (in particular of the protonation states) emphasise the importance in correctly describing ionisation states in modelling. The prediction of protonation states is possible through elaborated computational approaches. These calculations, however, are generally too demanding computationally for everyday modelling applications, in particular when analysing large databases in virtual screening. Locally induced dielectric fits determined by the protein environment can easily convert a non-charge assisted hydrogen bond into a salt bridge or a donor functional group into an acceptor group. Such ill-defined properties can easily mislead modelling approaches resulting in, e.g. incorrect binding modes and affinity scorings during docking. Accordingly, new fast methods must be developed that describe, at least approximately, the consequences of induced dielectric fits.

Experimental Section and Methods

Purification of the protein and ligand preparation

Bovine β-trypsin was used as commercially available from Merck and Sigma. Human α-thrombin was purchased from Enzyme Research Laboratories, Inc., South Bend, IN, and hirugen from American Diagnostica, Inc., Greenwich, CT. Bovine thrombin was purified through affinity chromatography. CH-Sepharose (Pharmacia Biotech) was activated through carbodiimide and coupled with hirudin HBW023. The column operated with 0.025 M sodium phosphate at pH 6.7, subsequently the same buffer with additional 0.3 M sodium chloride was used as eluant. The thrombin was eluted in the presence of benzamidine in phosphate buffer. After a further purification step on a gel column Sephadex G25, the protein solution was dialysed against water at 5 °C and freeze-dried. The activity of thrombin and trypsin was determined by active site titration with *p*-nitrophenyl guanidino-benzoate. The activity of bovine α-thrombin was 19 nmol/mg and of bovine β-trypsin 37.6 nmol/mg, respectively.

The inhibitors N^{α}-(2-naphthylsulphonyl)-L-3-amidino-phenylalanine-4′-methylpiperidide 1a, N^{α}-(2-naphthylsulphonyl-3-amidino-L-phenylalanine-D-pipecolinic acid 1b, N^{α}-(2-naphthylsulphonyl-3-amidino-L-phenylalanine-D-pipecolinic acid methylester 1bMe, N^{α}-(2-naphthylsulphonyl)-L-3-amidino-phenylalanine-isonipecotinic acid 1c, N^{α}-(2-naphthylsulphonyl)-L-3-amidino-phenylalanine-isonipecotinic acid methylester 1cMe, N^{α}-(2-naphthylsulphonyl)-3-amidino-L-phenylalanine-piperazide 1d and N^{α}-(2-naphthylsulphonyl)-3-amidino-L-phenylalanine-4′-acetyl-piperazide 1dAc were kindly provided by Pentapharm Ltd (Basel, Switzerland). The determination of the inhibition constants K_i (Tables 1 and 8) has been published.[58]

Napsagatran 2 and Napsagatran ester 2Et were kindly provided by Hoffmann-La Roche (Basel, Switzerland). CRC 220 3 was a kind gift from Chiron-Behring (Marburg, Germany). Inogatran 4[59] and melagatran 5[60] were provided by AstraZeneca (Mölndal, Sweden).

Isothermal titration calorimetry

Measurements were carried out using the MCS-ITC instrument from MicroCal (Northampton, USA).[11] In each experiment 0.2-0.4 mg bovine α-thrombin or 1.0-1.2 mg bovine β-trypsin, solvated in buffer solution, was placed in the 1.4 ml sample cell. In all cases, the reference cell contained demineralised water. All inhibitors were added to the protein solution by means of a 100 µl syringe. The ligand concentration was in the range of 0.14 mM up to 0.29 mM. The protein solution in the sample cell was stirred continuously during the entire experiment at 300 rpm. Data were evaluated using the ORIGIN 2.7 software as supplied with the instrument.

The standard buffer solution was composed of 50 mM buffer substance (Tris, Tris(hydroxymethyl)aminomethane; Tricine, *N*-tris(hydroxymethyl)methylglycine; Hepes, *N*-2-hydroxylethylpiperazine-*N'*-2-ethanesulphonic acid; pyrophosphate), 100 mM salt (sodium chloride, rubidium chloride) and 0.1 % (w/v) polyethylene glycol 8000, adjusted with hydrochloric acid, sodium chloride or potassium chloride to pH 7.8. Both the protein and the ligand solutions were degassed before measurement.

Potentiometric measurement of ionisation constants (pK_a)

Ionisation constants of several compounds were measured using the PCA 101-Partition Coefficient Analyser from Sirius Analytical Instruments (Forest Row, England). The silver-silver chloride pH electrode was calibrated using the FOUR-PLUS™ parameter standardisation. The aqueous sample solution of each inhibitor was adjusted to an ionic strength of 0.15 M potassium chloride. After adjusting to low pH with 0.5 N hydrochloric acid, titration followed with 0.5 N potassium hydroxide towards high pH. All measurements were carried out at 25 °C under argon atmosphere. The concentrations of the samples were in the range of 1 to 5 mM.

Data were analysed using difference curve fitting to approximate the pK_a values. They were subsequently refined using a non-linear least-squares procedure based on the software pK_alogP operated under Windows.

Crystallisation and structure analysis

Inhibitors were soaked into bovine β-trypsin or co-crystallized with β-trypsin at room temperature using vapour diffusion as described.[21,61] Crystals of trypsin grew within a few days in three different crystal forms (see Table 10). Hirugen-human-α-thrombin complex was prepared according to the method of Skrzypczak-Jankun *et al*.[62] and the sample was concentrated to 5.5 mg/ml. Crystallisation was carried out at 20 °C by vapour diffusion method using 24-30 % polyethylene glycol 4000 and 0.1 M sodium phosphate buffer (pH 7.3). Single crystals were soaked overnight in 30 % polyethylene glycol 4000, 0.1 M sodium phosphate buffer (pH 7.3), containing 0.5 mg/ml of inhibitor.

The inhibitors 1b, 3, 4 and 5 were co-crystallised with bovine β-trypsin. The protein concentration was 20 mg/ml, and the inhibitor concentrations varied between 1 and 10 mM. Crystals grew at pH 7 and pH 8 in 0.1 M imidazole and 0.1 to 0.3 M ammonium sulphate in the presence of 30 % polyethylene glycol 8000 within a few days. Inhibitors of limited solubility were dissolved initially in dimethylsulphoxide and subsequently diluted into aqueous solution.

The inhibitors 1cMe, 1d and 1dAc were soaked into β-trypsin. Their concentrations varied between 1 and 10 mM. Crystals for soaking procedure grew at pH 6 and pH 6.5 in 50 mM 2-(*N*-morpholino)ethanesulphonic acid and 1.9 M ammonium sulphate in presence of 25 mM benzamidine within one week. The trypsin crystals were harvested in 100 mM 2-(*N*-morpholino)ethanesulphonic acid and 2.5 M ammonium sulphate.

Data were collected using a RAXIS-IV image plate system on RIGAKU copper rotating anode generator (Molecular Structure Corporation) at 50kV and 100 mA and processed using DENZO.[63] The distance between crystal and detector was 100 mm. Images of 1° oscillation range, each within five to ten minutes, were collected at room temperature. Scaling and data reduction were performed with SCALEPACK[63] and the CCP4 program package.[64]

Starting coordinates for trypsin refinement were taken from the PDB entries 1MTS and 1MTV depending on the space group and cell constants; for thrombin, the hirugen-human-α-thrombin complex solved previously in our laboratory[65] were used. Conventional crystallographic refinement (rigid body, positional and temperature factor) was carried out using X-PLOR.[66] Inhibitors were constructed and minimised using SYBYL (Tripos Inc., St. Louis, USA), target bond lengths and angles used in the refinement of the complexes were those obtained after gradient minimisation in SYBYL. Model building was performed using O.[67] Data collection, processing and refinement statistics are given in Table 10. Selected electron densities are shown in Figure 13.

The coordinates of the crystal structure of Napsagatran 2 in complex with human thrombin were kindly provided by Hoffmann-la Roche, Basel.

The comparison of the complexes was performed by superimposing the coordinates of the amino acids of the catalytic triad His57, Asp102, Ser195 and Asp189 in the S1 specificity pocket. The modelling of the binding modes in thrombin (PDB code 1ETS) of inhibitors whose structures have only been solved in complex with trypsin were performed according to the same fitting protocol. None of the transferred inhibitors showed clashes with the thrombin surface.

Surface area calculations

The solvent accessible surfaces (Connolly surfaces) of thrombin, trypsin and their low molecular weight inhibitors were calculated by the procedure implemented in the software MS[68] with radii given by Bondi.[69] The polar surface portion included all nitrogen and oxygen atoms, whereas the non-polar surface area was constructed from the exposed sulphur, aliphatic and aromatic carbon atoms. The solvent accessible surface removed upon complex formation was determined as the difference between the surface of the complex and the sum of the surfaces of ligand and free protein based on crystal structures or, if no crystal structures were available, on the structures generated as described above.

Protein Data Bank accession numbers

Atomic coordinates have been deposited in the RCSB Protein Data Bank for publication (entry codes: trypsin: 1k1i (1b), 1k1j (1cMe), 1k1l (1d), 1k1m (1dAc), 1k1n (3), 1k1o (4), 1k1p (5); thrombin: 1k21 (4), 1k22 (5)).

Table 10. Crystallographic data and statistics of data collection

Compound	Space group	Cell constants						Resolution (Å)	R_{merge} (%)	Observed/unique reflection
		a(Å)	*b*(Å)	*c*(Å)	α(deg.)	β(deg.)	γ(deg.)			
1b-trypsin	$P2_12_12_1$	54.9	58.9	67.1	90	90	90	2.2	11.1	44,039/11,422
1cMe-trypsin	$P2_12_12_1$	62.9	68.9	63.6	90	90	90	2.2	13.0	47,705/14,388
1d-trypsin	$P2_12_12_1$	63.3	68.8	63.7	90	90	90	2.2	11.0	31,440/11,273
1dAc-trypsin	$P2_12_12_1$	63.5	68.9	63.8	90	90	90	2.2	22.1	38,834/12,028
3-trypsin	$P2_12_12_1$	54.8	58.3	67.3	90	90	90	2.0	14.7	82,823/14,371
4-trypsin	$P3_121$	55.2	55.2	109.7	90	90	120	2.0	7.1	50,017/12,832
5-trypsin	$P3_121$	55.6	55.6	110.2	90	90	120	1.9	12.0	63,590/15,363
4-thrombin	*C*2	69.7	71.5	71.9	90	100.0	90	1.86	5.4	22,3236/28,635
5-thrombin	*C*2	69.4	71.5	72.1	90	100.4	90	1.93	5.4	10,2503/25,984

Compound	*R*-factor (%)	Completeness(%)	Number of non-hydrogen atoms per asymmetric unit				rms deviation	
			Protein	Ions	Solvent	Inhibitor	Bond	Angles
1b	16.5	98.6	1629	Ca^{2+}	145	36	0.007	1.719
1cMe	16.8	98.4	1629	Ca^{2+}, SO_4^{2+}	115	37	0.008	1.801
1d	17.7	76.7	1629	Ca^{2+}, SO_4^{2+}	106	33	0.007	1.689
1dAc	16.3	81.4	1629	Ca^{2+}, SO_4^{2+}	127	36	0.007	1.672
3	16.8	94.8	1629	Ca^{2+}	140	42	0.008	1.842
4	16.5	93.9	1629	Ca^{2+}	179	31	0.008	1.833
5	17.0	94.7	1629	Ca^{2+}	180	31	0.007	1.789
4-thrombin	21.6	96.5	2239 (+37 dummy)	$2Na^+$; 28 sugar atoms	247	31	0.006	1.360
5-thrombin	19.7	99.4	2271 (+22 dummy)	$2Na^+$; 28 sugar atoms	239	31	0.006	1.295

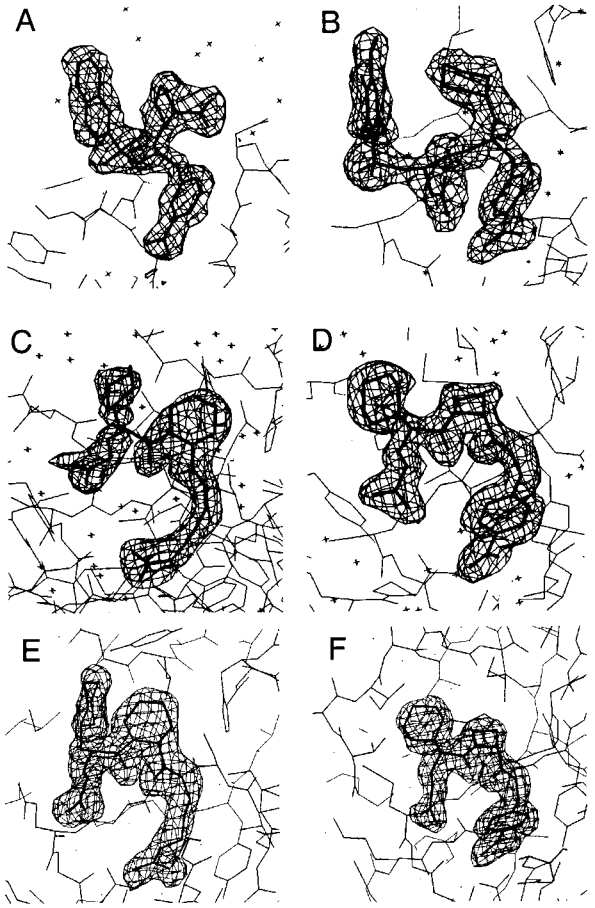

Figure 13. Experimental $2F_{obs} - F_{calc}$ electron densities of 1b (a), 3 (b), 4 (c) and 5 (d) with bovine β-trypsin, and 4 (e) and 5 (f) with human α-thrombin. The contour surface is at 0.9σ.

Acknowledgements

We acknowledge the help of Corinna Schraut (Philipps-University Marburg) in carrying out several thermodynamic measurements, of Gabriele Riesener (University of Jena) for her assistance in purifying thrombin and of Dr Holger Gohlke (Philipps-University Marburg) for calculating the solvent accessible surfaces. Samples of development compounds were kindly provided by Pentapharm Ltd (Basel, Switzerland), Hoffman-La Roche (Basel, Switzerland), Chiron-Behring (Marburg, Germany) and AstraZeneca (Mölndal, Sweden). We are particularly grateful to Dr Johanna Deinum (AstraZeneca) who communicated and discussed her thermodynamic studies on melagatran and inogatran to thrombin, which agree well with our results. A paper describing the studies of the group in Mölndal is in preparation. Parts of our work were presented at the 12th European QSAR Symposium, Copenhagen, Denmark, September 1998, and the 2nd International Conference on Applications of Biocalorimetry, Halle (Saale), Germany, March 1999.

References

1. Connelly, P. R. (1994). Acquisition and use of calorimetric data for prediction of the thermodynamics of ligand-binding and folding reaction of proteins. *Curr. Opin. Biotech.* **5**, 381-388.
2. Böhm, H. J. & Klebe, G. (1996). What can we learn from molecular recognition in protein-ligand complexes for the design of new drugs? *Angew. Chem. Int. Ed. Engl.* **35**, 2566-2587.
3. Dunitz, J. D. (1995). Win some, lose some: enthalpy-entropy compensation in weak intermolecular interactions. *Chem. Biol.* **2**, 709-712.
4. Davies, T. G., Hubbard, R. E. & Tame, J. R. H. (1999). Relating structure to thermodynamics: the crystal structures and binding affinity of eight OppA-peptide complexes. *Protein Sci.* **8**, 1432-1444.
5. Sleigh, S. H., Seavers, P. R., Wilkinson, A. J., Ladbury, J. E. & Tame, J. R. H. (1999). Crystallographic and calorimetric analysis of peptide binding to OppA protein. *J. Mol. Biol.* **291**, 393-415.
6. Hauptmann, J. & Stürzebecher, J. (1999). Synthetic inhibitors of thrombin and factor Xa: from bench to bedside. *Thromb. Res.* **93**, 203-241.
7. Ripka, W. C. (1997). New thrombin inhibitors in cardiovascular disease. *Curr. Opin. Chem. Biol.* **1**, 242-253.
8. Wiley, M. R. & Fisher, M. J. (1997). Small-molecule direct thrombin inhibitors. *Exp. Opin. Ther. Patents,* **7**, 1265-1282.
9. Liu, Y. & Sturtevant, J. M. (1995). Significant discrepancies between van't Hoff and calorimetric enthalpies. II. *Protein Sci.* **4**, 2559-2561.
10. Naghibi, H., Tamura, A. & Sturtevant, J. M. (1995). Significant discrepancies between van't Hoff and calorimetric enthalpies. *Proc. Natl Acad. Sci. USA,* **92**, 5597-5599.
11. Wiseman, T., Williston, S., Brandts, J. F. & Lin, L.-N. (1989). Rapid measurement of binding constants and heats of binding using a new titration calorimeter. *Anal. Biochem.* **179**, 131-137.
12. Ladbury, J. E. & Chowdhry, B. Z. (1998). *Biocalorimetry: Applications of Calorimetry in the Biological Sciences*, John Wiley & Sons, Chicester, England.
13. Bode, W., Turk, D. & Stürzebecher, J. (1990). Geometry of binding of the benzamidine- and argininebased inhibitors NAPAP and MQPA to human α-thrombin. X-ray crystallographic determination of the NAPAP-trypsin complex and modeling of NAPAP-thrombin and MQPA-thrombin. *Eur. J. Biochem.* **193**, 175-182.
14. Turk, D., Stürzebecher, J. & Bode, W. (1991). Geometry of the binding of the N^{α}-tosylated piperidides of *m*-amidino, *p*-amidino and *p*-guanidino phenylalanine to thrombin and trypsin. X-ray crystal structures of their trypsin complexes and modeling of their thrombin complexes. *FEBS Letters,* **287**, 133-138.
15. Reers, M., Koschinsky, R., Dickneite, G., Hoffmann, D., Czech, J. & Stüber, W. (1995). Synthesis and characterization of novel thrombin inhibitors based on 4-amidinophenylalanine. *J. Enzyme Inhib.* **9**, 61-72.
16. Gustafsson, D., Antonsson, T., Bylund, R., Eriksson, U., Gyzander, E., Nilsson, I. *et al.* (1998). Effects of melagatran, a new low-molecular-weight thrombin inhibitor, on thrombin and fibrinolytic enzymes. *Thromb. Haemost.* **79**, 110-118.
17. Nilsson, T., Sjöling-Erickson, A. & Deinum, J. (1998). The mechanism of binding of low-molecular-weight

active site inhibitors to human α-thrombin. *J. Enzyme Inhib.* **13**, 11-29.
18. Hilpert, K., Ackermann, J., Banner, D. W., Gast, A., Gubernator, K., Hadvary, P. *et al*. (1994). Design and synthesis of potent and highly selective thrombin inhibitors. *J. Med. Chem.* **37**, 3889-3901.
19. Christensen, J. J., Hansen, L. D. & Izatt, R. M. (1976). *Handbook of Proton Ionization Heats and Related Thermodynamic Quantities*, John Wiley and Sons, New York.
20. Fukada, H. T. & Takahashi, K. (1998). Enthalpy and heat capacity changes for the proton dissociation of various buffer components in 0.1 M potassium chloride. *Proteins: Struct. Funct. Genet.* **33**, 159-166.
21. Renatus, M., Bode, W., Huber, R., Stürzebecher, J. & Stubbs, M. T. (1998). Structural and functional analyses of benzamidine-based inhibitors in complex with trypsin: implications for the inhibition of factor Xa, tPA and urokinase. *J. Med. Chem.* **41**, 5445-5456.
22. Bergner, A., Bauer, M., Brandstetter, H., Stürzebecher, J. & Bode, W. (1995). The X-ray crystal structure of thrombin in complex with N^{α}-2-naphthylsulfonyl-L-3-amidino-phenylalanyl-4-methylpiperidide: the beneficial effect of filling out an empty cavity. *J. Enzyme Inhib.* **9**, 101-110.
23. Banner, D. W. & Hadvary, P. (1991). Crystallographic analysis at 3.0 Å resolution of the binding to human thrombin of four active site-directed inhibitors. *J. Biol. Chem.* **266**, 20085-20093.
24. Brandstetter, H., Turk, D., Hoeffken, W., Grosse, D., Stürzebecher, J., Martin, P. D. *et al*. (1992). Refined 2.3 Å X-ray crystal structure of bovine thrombin complexes formed with the benzamidine and arginine-based thrombin inhibitors NAPAP, 4-TAPAP and MQPA. A starting point for improving antithrombotics. *J. Mol. Biol.* **226**, 1085-1099.
25. Stürzebecher, J., Walsmann, B., Voigt, B. & Wagner, G. (1984). Inhibition of bovine and human thrombins by derivatives of benzamidine. *Thromb. Res.* **36**, 457-465.
26. Gómez, J. F. & di Cera, E. (1995). Thermodynamic mapping of the inhibitor site of the aspartic protease endothiapepsin. *J. Mol. Biol.* **252**, 337-350.
27. Baker, B. M. & Murphy, K. P. (1996). Evaluation of linked protonation effects in protein binding reactions using isothermal titration calorimetry. *Biophys. J.* **71**, 2049-2055.
28. Doyle, M. L. (1997). Characterization of binding interactions by isothermal titration calorimetry. *Curr. Opin. Biotech.* **8**, 31-35.
29. Tame, J. R. H. (1999). Scoring functions: a view from the bench. *J. Comp. Aided Mol. Des.* **13**, 99-108.
30. Perozzo, R., Jelesarov, I., Bosshard, H. R., Folkers, G. & Scapozza, L. (2000). Compulsory order of substrate binding to herpes simplex virus type 1 thymidine kinase. *J. Biol. Chem.* **275**, 16139-16145.
31. Jelesarov, I. & Bosshard, H. R. (1999). Isothermal titration calorimetry and differential scanning calorimetry as complementary tools to investigate the energetics of biomolecular recognition. *J. Mol. Recognit.* **12**, 3-18.
32. Böhm, H. J., Brode, S., Hesse, U. & Klebe, G. (1996). Oxygen and nitrogen in competitive situations: which is the hydrogen-bond acceptor? *Chem. Eur. J.* **2**, 1509-1513.
33. Edsall, J. T. (1935). Apparent molal heat capacities of amino acids and other organic compounds. *J. Am. Chem. Soc.* **57**, 1506-1507.
34. Connelly, P. R. & Thompson, J. A. (1992). Heat capacity changes and hydrophobic interactions in the binding of FK506 and rapamycin to the FK506 binding protein. *Proc. Natl Acad. Sci. USA,* **89**, 4781-4785.
35. Privalov, P. L. & Gill, S. J. (1988). Stability of protein structure and hydrophobic interaction. *Advan. Protein Chem.* **39**, 191-234.
36. Sturtevant, J. M. (1977). Heat capacity and entropy changes in processes involving proteins. *Proc. Natl Acad. Sci. USA,* **74**, 2236-2240.
37. Spolar, R. S. & Record, M. T. (1994). Coupling of local folding to site-specific binding of proteins to DNA. *Science,* **263**, 777-784.
38. Makhatadze, G. I. & Privalov, P. L. (1990). Heat capacity of proteins: I. Partial molar heat capacity of individual amino acid residues in aqueous solution: hydration effect. *J. Mol. Biol.* **213**, 375-384.
39. Makhatadze, G. I. & Privalov, P. L. (1993). Contribution of hydration to protein folding thermodynamics. I. The enthalpy of hydration. *J. Mol. Biol.* **232**, 639-659.
40. Privalov, P. L. & Makhatadze, G. I. (1993). Contribution of hydration to protein folding thermodynamics. II. The entropy and Gibbs energy of hydration. *J. Mol. Biol.* **232**, 660-679.
41. Xie, D. & Freire, E. (1994). Molecular basis of cooperativity in protein folding. V. Thermodynamics and structural conditions for the stabilization of compact denatured states. *Proteins: Struct. Funct. Genet.* **19**, 291-301.
42. Murphy, K. P., Bhakuni, V., Xie, D. & Freire, E. (1992). Molecular basis of co-operativity in protein folding. III. Structural identification of cooperative folding units and folding intermediates. *J. Mol. Biol.* **227**, 293-306.
43. Murphy, K. P. & Freire, E. (1992). Thermodynamics of structural stability and cooperative folding behavior in proteins. *Advan. Protein Chem.* **43**, 313-361.
44. Spolar, R. S., Ha, J. H. & Record, M. T., Jr (1989). Hydrophobic effect in protein folding and other noncovalent processes involving proteins. *Proc. Natl Acad. Sci. USA,* **86**, 8382-8385.
45. Spolar, R. S., Livingstone, J. R. & Record, M. T., Jr (1992). Use of liquid hydrocarbon and amide transfer data to estimate contributions to thermodynamic fuinctions of protein folding from the removal of nonpolar and polar surface from water. *Biochemistry,* **31**, 3947-3955.
46. Liggins, R. J. & Privalov, P. L. (2000). Energetics of the specific binding interaction of the first three zinc finders of the transcription factor TF IIA with its cognate DNA sequence. *Proteins: Struct. Funct. Genet.* **4**, 50-62.
47. Dunitz, J. D. (1994). The entropic cost of bound water in crystals and biomolecules. *Science,* **264**, 670.
48. Wells, C. M. & di Cera, E. (1992). Thrombin is a Na^+-activated enzyme. *Biochemistry,* **31**, 11721-11730.
49. Ayala, Y. & di Cera, E. (1994). Molecular recognition by thrombin: role of the slow → fast transition, site-specific ion binding energetics and thermodynamic mapping of structural components. *J. Mol. Biol.* **235**, 733-746.
50. di Cera, E., Guinto, E. R., Vindigni, A., Dang, Q. D., Ayala, Y. M., Wuyi, M. & Tulinsky, A. (1995). The Na^+ binding site of thrombin. *J. Biol. Chem.* **270**, 22089-22092.

51. Zhang, E. & Tulinsky, A. (1997). The molecular environment of the Na^+ binding site of thrombin. *Biophys. Chem.* **63**, 185-200.
52. Engh, R., Brandstetter, H., Sucher, G., Baumann, U., Kühne, A., Eichinger, A. *et al*. (1996). Enzyme flexibility, solvent and ''weak'' interactions characterize thrombin-ligand interactions: implications for drug design. *Structure,* **15**, 1353-1362.
53. van de Locht, A., Bode, W., Huber, R., Le Bonniec, B. F., Stone, S. R., Esmon, C. T. & Stubbs, M. T. (1997). The thrombin E192Q:BPTI-complex reveals gross structural rearrangements: implications for the interaction with antithrombin. *EMBO J.* **16**, 2977-2984.
54. Ayala, Y. M., Vindigni, A., Nayal, M., Spolar, R., Record, M. T. & di Cera, E. (1995). Thermodynamic investigations of hirudin binding to the slow and fast forms of thrombin: evidence for folding transitions in the Inhibitor and protease coupled to binding. *J. Mol. Biol.* **253**, 787-798.
55. Rydel, T. J., Tulinsky, A., Bode, W. & Huber, R. (1991). Refined structure of the hirudin-thrombin complex. *J. Mol. Biol.* **221**, 583-601.
56. Stubbs, M. T. & Bode, W. (1993). A player of many parts: the spotlight falls on thrombin's structure. *Thromb. Res.* **69**, 1-58.
57. Guinto, E. R. & di Cera, E. (1996). Large heat capacity change in a protein-monovalent cation interaction. *Biochemistry,* **35**, 8800-8804.
58. Stürzebecher, J., Prasa, D., Wikström, P. & Vieweg, H. (1995). Structure-activity relationships of inhibitors derived from 3-amidinophenylalanine. *J. Enzyme Inhib.* **9**, 87-99.
59. Teger-Nilsson, A. C. E. & Bylund, R. E. (1993). Preparation of peptide derivatives as thrombin inhibitor, PCT Int. Appl. WO 93/11152.
60. Antonsson, K. T., Bylund, R. E., Gustafsson, N. D. & Nilsson, N. O. I. (1994). Trypsin-like protease-inhibiting peptide derivatives, their synthesis and therapeutic use, PCT Int. Appl. WO 94/29336.
61. Stubbs, M. T., Huber, R. & Bode, W. (1995). Crystal structures of factor Xa specific inhibitors in complex with trypsin: structural grounds for inhibition of factor Xa and selectivity against thrombin. *FEBS Letters,* **375**, 103-107.
62. Skrzypczak-Jankun, E., Carperos, V., Ravichandran, K. G., Tulinsky, A., Westbrook, M. & Maraganore, J. (1991). The structure of the hirugen and hirulog 1 complexes of α-thrombin. *J. Mol. Biol.* **221**, 1379-1393.
63. Otwinowski, Z. & Minor, W. (1997). Processing of X-ray diffraction data collected in oscillation mode. *Methods Enzymol.* **276**, 307-326.
64. CCP4 (1994). The CCP4 suite: programs for protein crystallography. *Acta Crystallog. sect. D,* **50**, 760-763.
65. Nöteberg, D., Brånalt, J., Kvarnström, I., Linschoten, M., Musil, D., Nyström, J.-E. *et al*. (2000). New proline mimetics: Synthesis of thrombin inhibitors incorporating cyclopentane- and cyclopentenedicarboxylic acid templates in the P2 position. Binding conformation investigated by X-ray crystallography. *J. Med. Chem.* **43**, 1705-1713.
66. Brünger, A. (1992). *X-PLOR (Version 3.1). A system for X-ray Crystallography and NMR*, Yale University Press, New Haven, CT.
67. Jones, T. A., Zou, J. Y., Cowan, S. W. & Kjeelgaard, M. (1991). Improved methods for building protein models in electron density maps and location of errors in these models. *Acta Crystallog.* **5**, 802-810.
68. Connolly, P. R. (1983). Solvent accessible surfaces of proteins and nucleic acids. *Science,* **221**, 709-713.
69. Bondi, A. (1968). *Physical Properties of Molecular Crystals, Liquids and Glasses*, John Wiley & Sons Inc., New York, USA.

Edited by R. Huber

(Received 15 May 2001; received in revised form 3 September 2001; accepted 3 September 2001)